acp-2016-617: Review #1

"Surface ozone in the southern hemisphere: 20 years of data from a site with a unique setting in El Tololo, Chile" by J. G. Anet et al.

We would like to thank the anonymous referee #1 for his/her great review of our publication. Below, we provide the answers to his/her comments.

Section 1 - Introduction: For the discussion about the seasonal cycle of tropospheric ozone with maximum in spring or in summer Cooper et al., 2014 (section 4) showing seasonal cycle by hemisphere with a maximum in spring for the south hemisphere using OMI/MLS tropospheric column ozone should be cited.

We added following sentence in the "introduction", Page 3, L20: "*These findings were more broadly confirmed by Cooper et al. (2014), who, using satellite-measured total column ozone datasets, classified the onsets of the Total Column Ozone (TCO) maxima globally. In general, spring TCO maxima are found rather on the SH, while summer TCO maxima are prominent in the NH.*"

Section 3.3 - Methods: Is it possible to further justify the 4 ppbv threshold used to exclude high changes between one hour and the next?

The 4 ppb limit has been defined after thorough trial-and-error experiments. Those 4 ppb created least "false negatives" or "false positives" during automatic filtering, which otherwise would have to be corrected manually. This value changes from station to station, as it depends from the natural ozone variability. We added the following to the paper: "*This value of 4 ppb has been defined as such to avoid too many false positives or negatives during the automatic filtering process, in order to minimize the workload during the manual dataset review process.*"

Section 3.3 - Methods: Would the authors confirm that 8.9% represents data influenced by local pollution and missing data? Does it give a first element that ozone at El Tololo is unlikely driven by local pollution?

Thank you for this valuable comment. The reviewer is right that the 8.9% do cover both the excluded data by the filtering process as well as missing data. This number is dominated by the larger data gaps (see grey periods in Fig. 4 and Table S1) and thus, does not give neither a meaningful impression of the rigor of the filter nor of the frequency of rare events of local pollution. The filtering process only excludes 4.9% from the available data. This information will be added to the manuscript. Indeed, a fraction of only 4.9% being identified as influenced by local pollution is a first benchmark indicating the pristine setting of the station. It is worth to mention that it is generally difficult to unambiguously

classify data points as “local pollution events” or “regional pollution events” as periods with steadily elevated mole fractions would not be excluded by the filter. However, the absence of frequent local emissions (e.g. due to the operation of the back-up diesel generator or heavy traffic on the Cerro Tololo premises) is also in line with the observations of the station operators. Therefore, we rephrased the respective sentence that it reads: "*The filtering of the data excludes approximately 4.9% of the available data indicating the pristine setting of the sampling site with hardly any influence from local pollution sources from the premises' infrastructure.*"

Section 3.3 - Methods: Make clear that the trajectories data set are provided by Skerlak et al.

In order to avoid any misunderstanding, following sentence was reformulated: "*Driven by the wind field of ERAI, Škerlak (2014) calculated kinematic trajectories using an 3-steps iterative Eulerian integration scheme (Sprenger and Wernli, 2015).*"

Section 3.3 - Methods: Would the authors write the definition of the max flux more explicitly as a mathematical formulae? That would be easier for the reader.

Thanks for this good suggestion. We adapted the manuscript accordingly: $\Delta MF_{O_3} \approx n * t * \Delta m_{O_3}$

Section 4.1 - Trends: the authors are using Figure 10 […] to argue in favor of the role of ozone STE max flux in tropospheric ozone seasonal changes and changes in time. This paragraph needs to be clarified. The time periods used to assess the changes of the seasonal cycle of tropospheric ozone over time are 1996-2000 and 2011-2015, whereas the time period in Figure 10 ends in 2013. The shift of ozone maximum from October to August seems to be seen on Figure 10 but not on Figure 5, why?

I would suggest to add the specific humidity in the study. It can be added on Figure 10 and its seasonal cycle could be shown as well. It will give more evidence of the impact of stratospheric ozone on tropospheric ozone changes.

The reviewer's interpretation is totally comprehensible and we would like to clarify certain points. First, the period shown in Fig. 10 runs only from 1997 to 2013, i.e. no data are shown for 1995, 1996, 2014 and 2015, due to the way the analysis routine works. The intrinsic mode functions (IMF) was calculated for 4 year sliding windows, therefore “cutting” the first and last two years. Calculating the IMF over yearly data would lead to less meaningful/representative results due to the relatively low signal-to-noise-ratio (interannual variability). The shift of the timing in the maximum of ozone is less visible in Figure 5 also due to the different data treatment. Figure 5 shows a comparison of 3 different percentiles of 5-year-monthly averages, not absolute maximal values, and data are aggregated in monthly bins. We appreciate the suggestion to use specific humidity. Usually, ozone peaks associated with stratospheric intrusions are mostly accompanied with low relative humidity (RH) as it was also

shown by Rondanelli et al. (2002) for El Tololo. We also looked into the RH measurements. Unfortunately, the RH time series at El Tololo suffers from sensor deterioration which jeopardizes a detailed inclusion of the RH data into the analysis (see Fig. S7 c).

In order to help the reader to interpret the Figures, we changed the manuscript, the caption of Figure 9 and the text (see Section 4.3 of the revised manuscript) as following: "*For calculation, a 4-year sliding window of daily data was defined and run over all data between 1996 and 2015.*"

And: "*Note that the regression is only poorly visible in Fig. 5, in which data are aggregated in monthly bins and a comparison of 3 different percentiles of 5-year-monthly averages, instead of absolute maximal values, is shown.*"

And: "*A 4-year sliding window of daily data was applied. Average values for the years 1996-1999 are shown as the data point in end of December 1997, 1997-2000 in end of December 1998, and so forth until years 2012-2015 which are shown as data point in end of December 2013.*" was added to the caption of Figure 9.

Section 4.1 - Trends: The authors are pointing out a shift of two months between maximum of STE flux (Figure A9) and maximum of ozone mixing ratio (Figure 5). This is true for the time period 2011-2015 but not for 1996-2000. In 1996-2000, the STE max flux shows two maxima. This paragraph needs to be clarified.

Thanks for this remark. It is true that the STE trajectory frequency of the earlier period shows two maxima. We erroneously focused purely on the more recent period. The finding of the two maxima (or rather: the persistent low in August) in the 1996-2000 period is robust and can be found in the absolute maxima, mean, median and 5-95 percentiles. The reason for this finding is not entirely clear – we assume that the state of the QBO and ENSO might have played an important role on STE during this period (relatively strong El Niño, weaker la Niña), as shown in Neu et al. (2014). As can be seen in Fig. 1R1 and Fig. 2R1 (below), the QBO shear index (QBO, red lines) and the multivariate ENSO index (MEI, blue lines) where in-phase during nearly two years between 1996-2000 and relatively out-of-phase during 2011-2015. The effects are known: the tropical upwelling increases, boosting the planetary-scale wave activity and henceforth the stratospheric circulation, finally leading to an increase in STE exchange in the sub- and extratropics (Neu et al. 2014 & references therein). This most likely leads to an overall stronger STE activity especially in JJA 1997 and JJA 1998. Also due to the comments of reviewer #2, we have entirely reformulated section 4.3

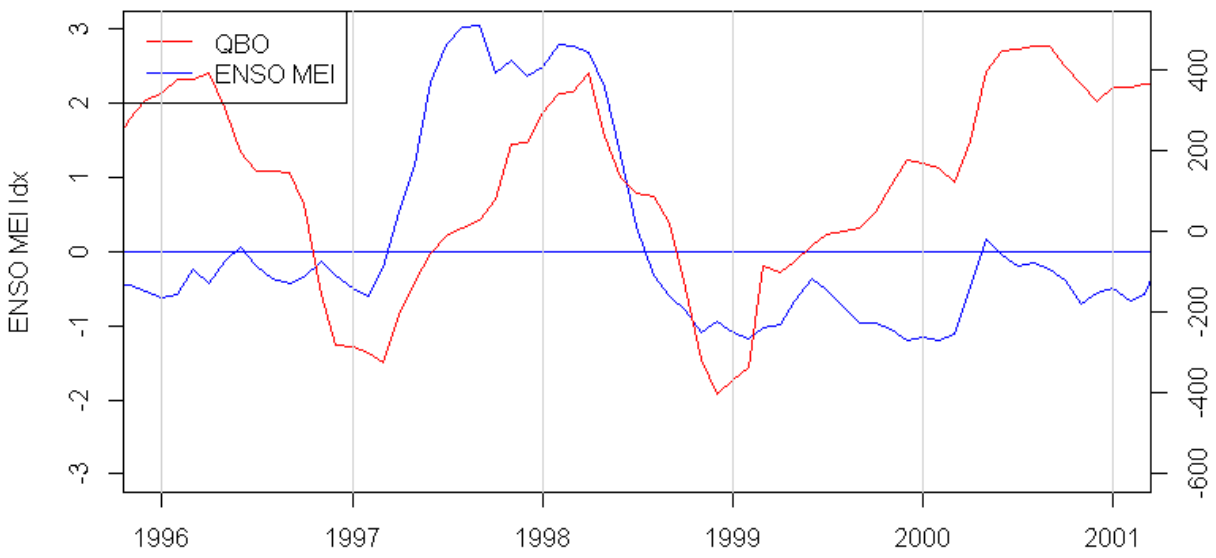

Fig. 1R1: ENSO MEI (blue) and QBO shear index (red) for the 1996-2000 period.

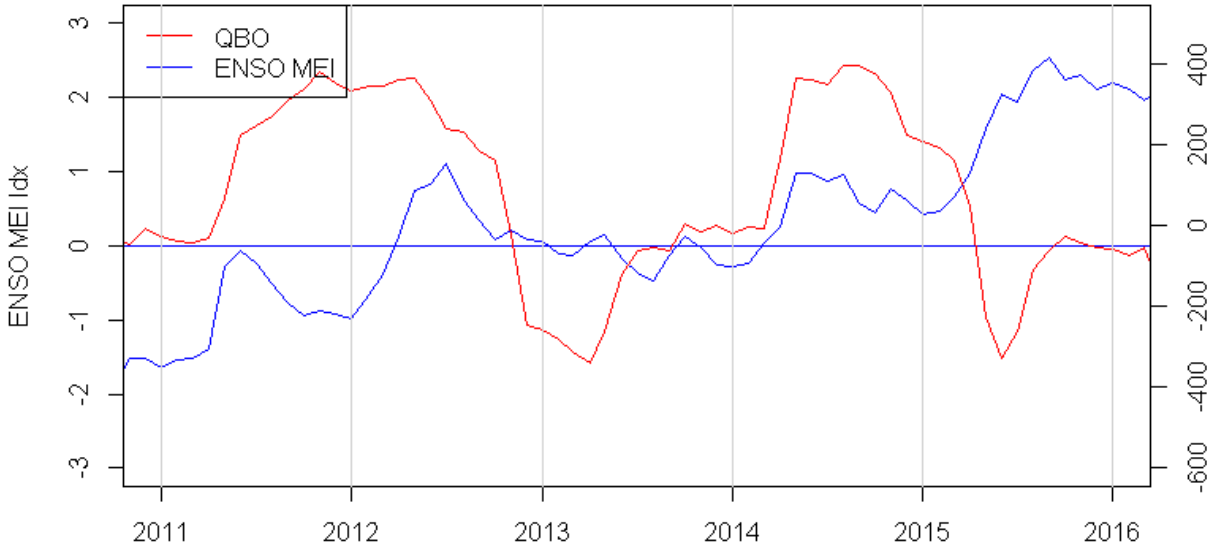

Fig. 2R1: ENSO MEI (blue) and QBO shear index (red) for the 2011-2015 period

Section 4.1 - Trends: Factors influencing the trend in austral fall could be biomass burning in Australia and south of Africa (Cooper et al., 2014), more than Southeast Asia as biomass burning in this region occur mostly in the northern hemisphere.

This is correct. However, by austral fall, the Southeast-Asian branch of the ITCZ has already moved northwards, allowing first pollutants to be transported southbound of the ITCZ into the southern hemisphere. Moreover, biomass burning emissions in Australia and Southern Hemisphere Africa are minimal in austral fall (van der Werf et al., 2006). For clarity, we rewrote the following in Section 4.3 of the revised manuscript: "*An increase of biomass burning in Southeast Asia (e.g. Shi and Yamaguchi, 2014;Verma et al., 2015) and Australia (Cooper et al., 2014) with subsequent eastward transport of ozone precursors, could also explain the positive anomaly in MAM in the 2011-2015 period, as the Northward*

migration of the ITCZ during this time of the year starts to allow effects of NH emissions to be seen in the SH and prevailing westerly conditions (see Fig. 2) exclude any sensitivity of ozone mole fractions at TLL to emissions on the South American continent."

Section 4.3 - Large-Scale influences at TLL: As said above, Figure 10 shows time series from 1996 to 2013 and not 2015. Would it be possible to extent the time period to 2015?

As replied above, this is technically not possible.

Section 4.3 - Large-Scale influences at TLL: The shift in the seasonal cycle has been discussed in section 4.1 - Trends. I would suggest to move the paragraph of the section 4.1 to the section 4.3, otherwise it is confusing for the reader.

This is a very good idea. We moved paragraph "seasonal cycles" in 4.1. to 4.3 and, together with the remarks of reviewer #2, restructured and reformulated the section extensively.

Section 4.3 - Large-Scale influences at TLL: Instead of discuss the relative humidity, I would suggest to discuss the specific humidity which is the absolute value of humidity in the air.

As said above, we could only base ourselves on some very short RH measurements done at TLL, as the sensors mostly were reporting wrong values. Since 2014, the station has been equipped with new sensors, and we totally agree that such a study, relating tropospheric ozone with specific humidity, should absolutely be carried out in near future.

Figures 8 and 10: on the y or x-axis, I would suggest to give the month associated to the given week or day of the year. It will help the reader to follow the analysis which is often based on season or month in the text.

We agree that the reader could be helped by completing the y-axis of Figure 10 with months: We have therefore adapted Figure 10 as the reviewer suggested:

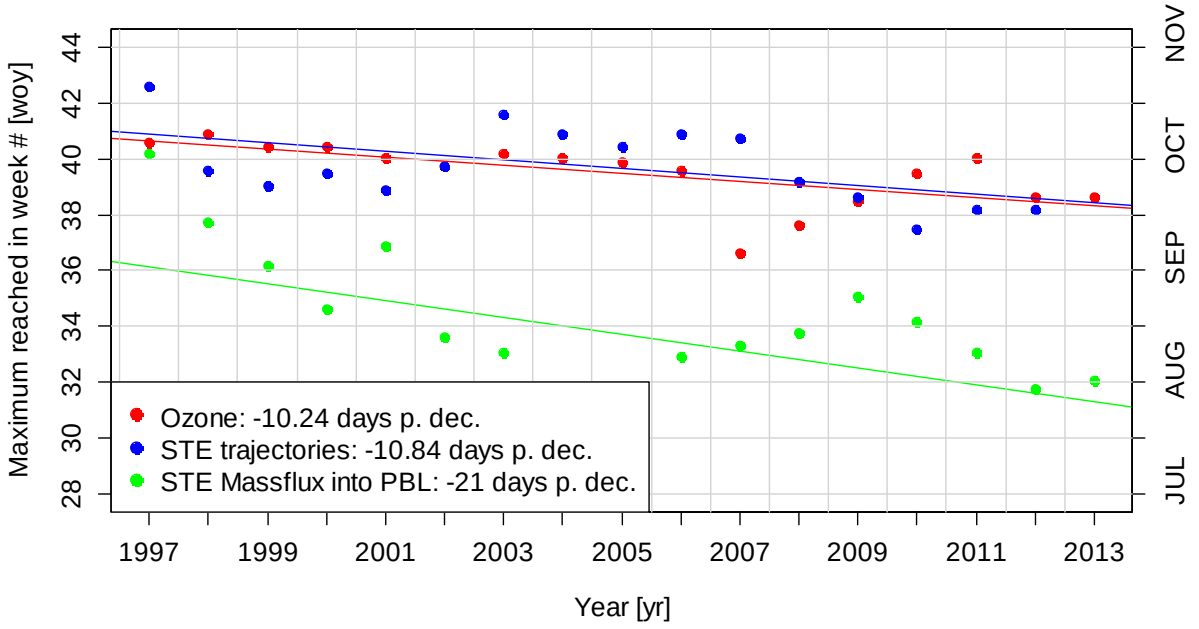

Fig. 3R1: Revised Fig. 10 of original manuscript

Table 1: I would suggest to add the 95% confidence limit and the p-value

We added the 95% confidence limit and the p-value in Table 1 as suggested. On the same time, we slightly revised the numbers as we updated the analysis routine. The latter finding nevertheless does not influence the overall trend discussion.

Typos/Technical corrections

I would suggest to add the longitude and latitude of El Tololo in the title

We agree this would be a good idea. We therefore revised the title: *Surface ozone in the southern hemisphere: 20 years of data from a site with a unique setting in El Tololo, Chile, 30°N, 71°W, 2200 m asl*

L.5 p.3: Change "Unites" to "United"

L.8 p.7: Change "Stratosphere-Troposphere-Transport" to "Stratosphere Troposphere-Exchange"

L.19-20 p.9: I would link both paragraphs (no enter)

L.22 p.9: Change "positive deviations" to "increase"

L.23 p.9: Change "During the remaining of the year" to "For the other months of the year"

We adopted the suggested changes.

L.29 p.9: I would suggest to remove "The attentive reader may have realized that" and start the sentence directly by "The maximum of STE…"

We agree that this makes the text more readable and adapted the manuscript.

L.30 p.9: Change "ration" to "ratio" - L.13 p.10: "biomass burning in …" a word is missing?

We corrected the typos

L.29 to 30 p.: I would suggest to remove this paragraph as everything is already written in the caption of the figure

We assumed that the reviewer meant L29-30 p11, and we have removed the double information from the text about Fig. 8.

Figure 3: I would suggest to change "(a&b)" to "(a) DJF, b) JJA)", same for "(c & d)" and "(e & f)"

Good idea, we changed the figure caption accordingly.

Figure 4: I would suggest to add minor ticks to show all the years - Figure 5: I would suggest to add minor ticks to show all the months

We modified the figures, adding the minor ticks:

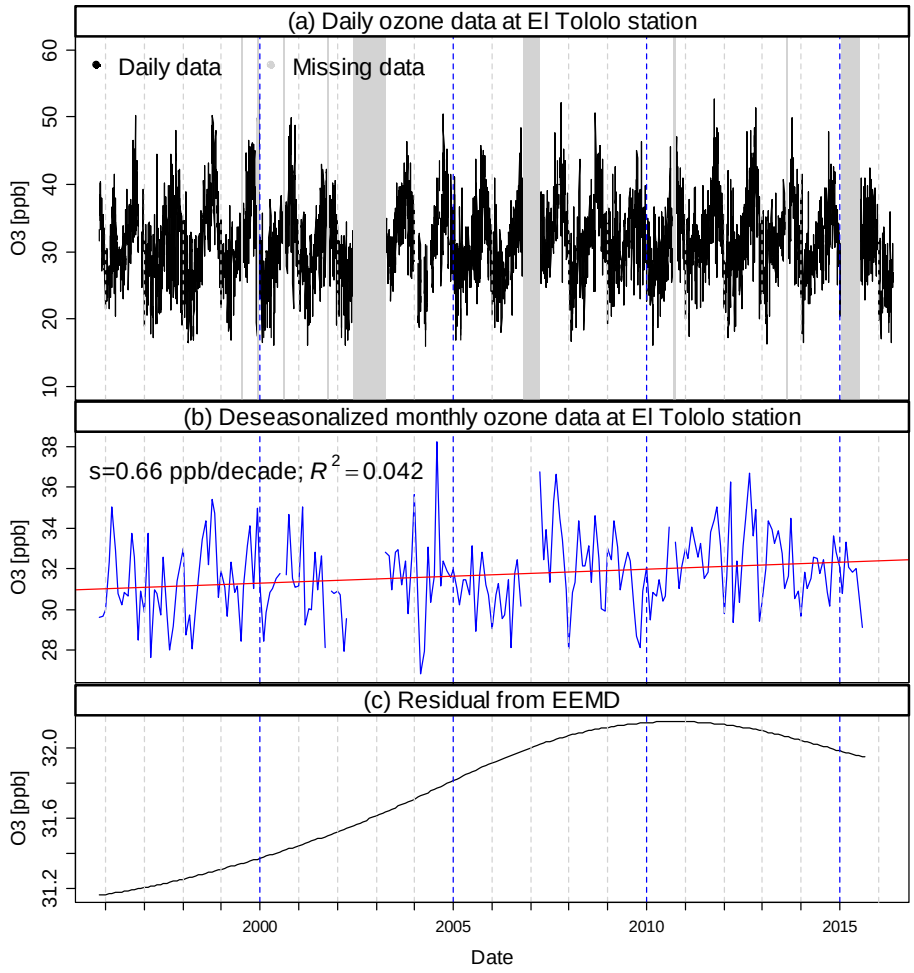

Fig. 4R1: Revised Fig. 4 of original manuscript

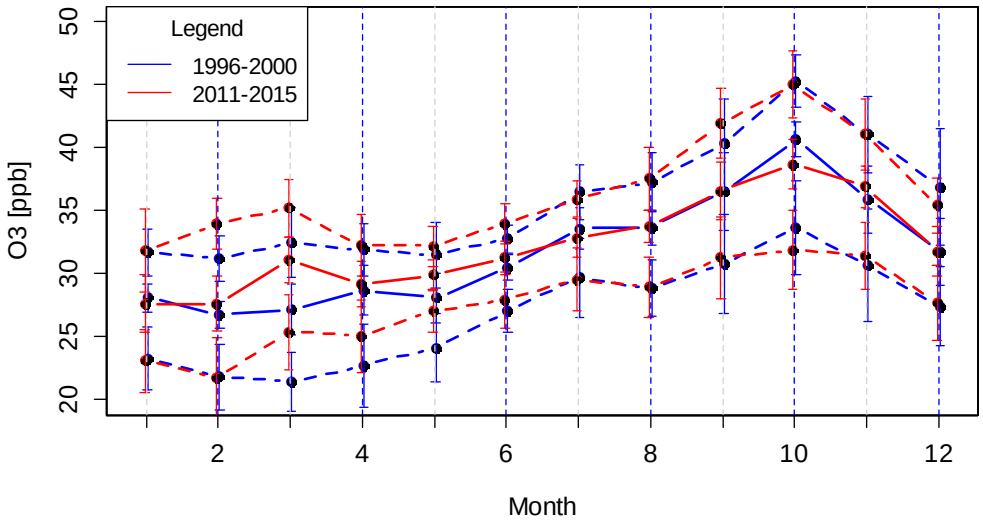

Fig. 5R1: Revised Fig. 5 of original manuscript

Figure A4: I would suggest to change the caption of the figures in order to have the consistent name of the season related to the month: Fall (MAM). It is quite common to order the season as followed: winter, spring, summer, and fall

We modified the figure caption accordingly, as well as the order:

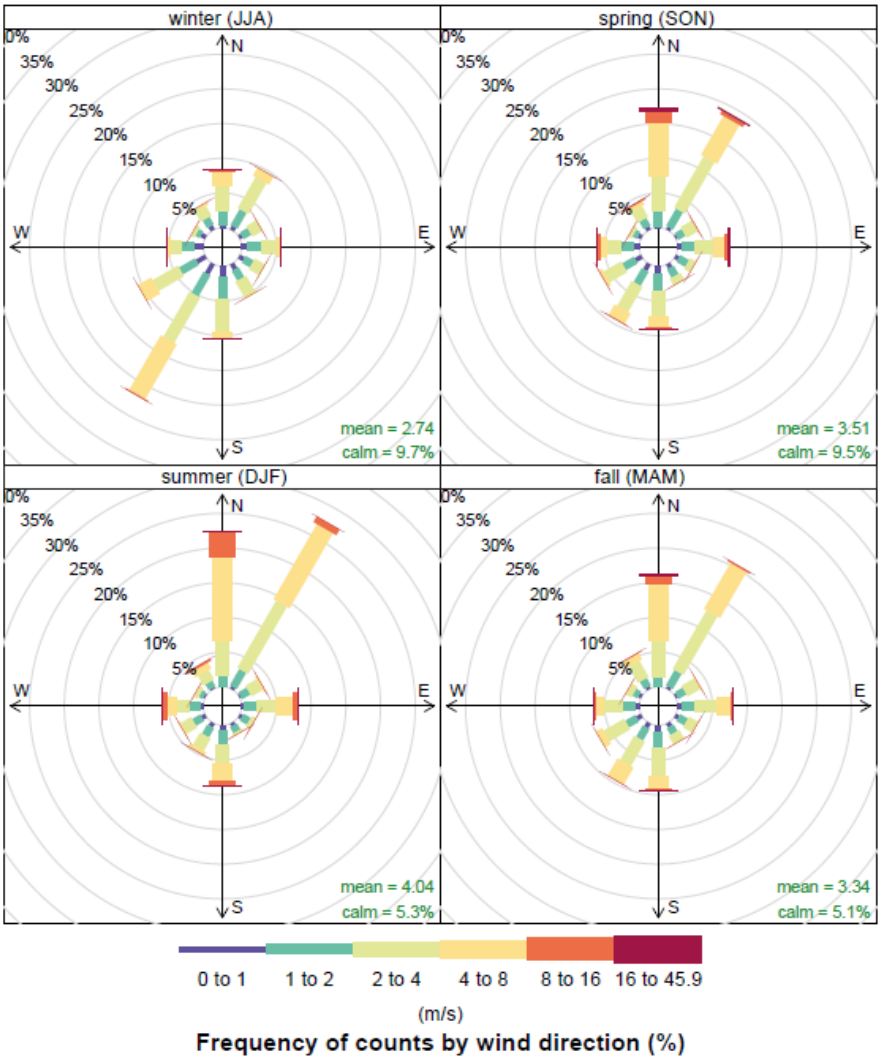

Fig. 6R1: Revised Fig. A4 of original manuscript

Figure A6: I would suggest to follow the common order: winter (JJA), spring (SON), summer (DJF), and fall (MAM)

We reordered the seasons following the suggestion of the reviewer.

Figure A7: I would suggest to add dash lines for the three panels as in Figure 4 and add minor ticks to show all the years

We adapted the minor ticks on the x-axis as suggested:

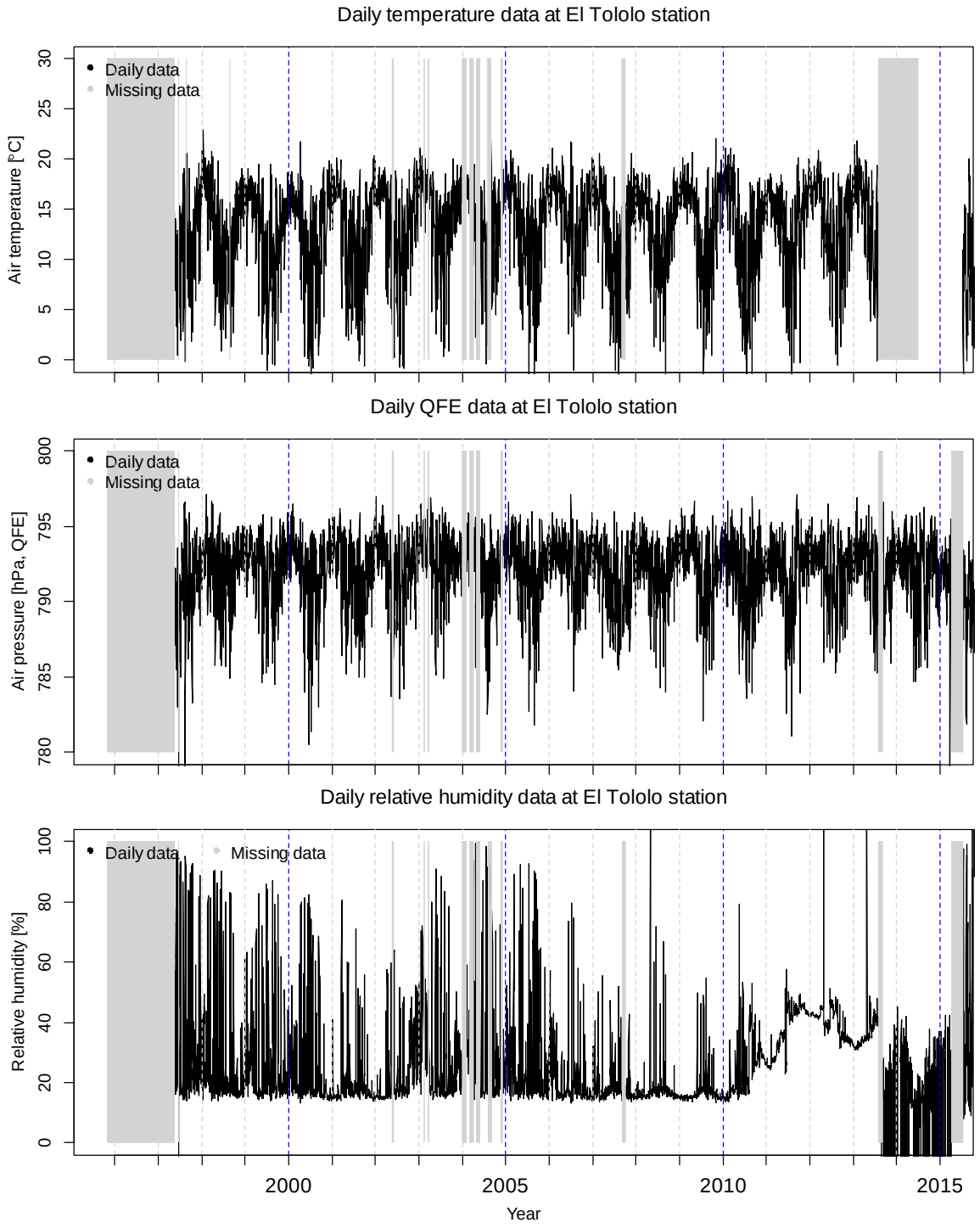

Fig. 7R1: Revised Fig. A7 of original manuscript

Figure A9: I would suggest to add minor ticks to show all the month - In general be careful with the use of "STE" and "STT". STE = stratosphere - troposphere exchange, STT = stratosphere to troposphere transport

Thanks for pointing out the wrong naming. We modified the figure caption and added minor ticks:

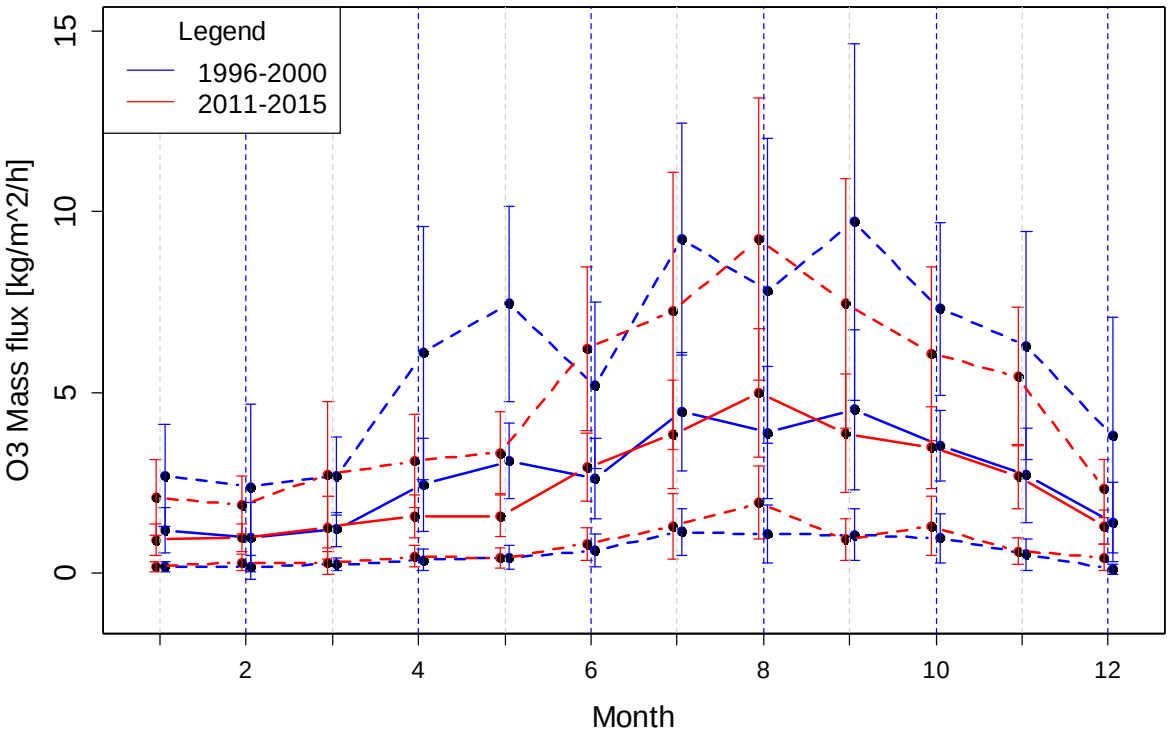

Fig. 8R1: Revised Fig. A9 of original manuscript; Caption modified to: *Mean annual ozone STE mass flux cycle (1995-2000 and 2010-2015) showing mean, upper 95th percentile and lower 5th percentile*

References

Cooper, O. R., Parrish, D. D., Ziemke, J., Balashov, N. V., Cupeiro, M., Galbally, I. E., Gilge, S., Horowitz, L., Jensen, N. R., Lamarque, J. F., Naik, V., Oltmans, S. J., Schwab, J., Shindell, D. T., Thompson, a. M., Thouret, V., Wang, Y., and Zbinden, R. M.: Global distribution and trends of tropospheric ozone: An observation-based review, Elementa: Science of the Anthropocene, 2, 000029-000029, 10.12952/journal.elementa.000029, 2014.

Neu, J. L., Flury, T., Manney, G. L., Santee, M. L., Livesey, N. J., and Worden, J.: Tropospheric ozone variations governed by changes in stratospheric circulation, Nature Geosci, 7, 340-344, 10.1038/ngeo2138, 2014.

Rondanelli, R., Gallardo, L., and Garreaud, R. D.: Rapid changes in ozone mixing ratios at Cerro Tololo (30°10′S, 70°48′W, 2200 m) in connection with cutoff lows and deep troughs, Journal of Geophysical Research: Atmospheres, 107, 1-15, 10.1029/2001JD001334, 2002.

Shi, Y., and Yamaguchi, Y.: A high-resolution and multi-year emissions inventory for biomass burning in Southeast Asia during 2001–2010, Atmospheric Environment, 98, 8-16, http://dx.doi.org/10.1016/j.atmosenv.2014.08.050, 2014.

Škerlak, B.: Climatology and process studies of tropopause folds , cross-tropopause exchange , and transport into the boundary layer, Dissertation, ETH ZURICH, 2014.

Sprenger, M., and Wernli, H.: The LAGRANTO Lagrangian analysis tool – version 2.0, Geosci. Model Dev., 8, 2569-2586, 10.5194/gmd-8-2569-2015, 2015.

van der Werf, G. R., Randerson, J. T., Giglio, L., Collatz, G. J., Kasibhatla, P. S., and Arellano, a. F.: Interannual variability of global biomass burning emissions from 1997 to 2004, Atmospheric Chemistry and Physics Discussions, 6, 3175-3226, 10.5194/acpd-6-3175-2006, 2006.

Verma, S. K., Kawamura, K., Chen, J., Fu, P., and Zhu, C.: Thirteen years of observations on biomass burning organic tracers over Chichijima Island in the western North Pacific: An outflow region of Asian aerosols, Journal of Geophysical Research: Atmospheres, 120, 4155-4168, 10.1002/2014JD022224, 2015.

acp-2016-617: Review #2

"Surface ozone in the southern hemisphere: 20 years of data from a site with a unique setting in El Tololo, Chile" by J. G. Anet et al.

We would like to thank the anonymous referee #2 for his/her critical review of our publication. Below, we provide the answers to his/her comments.

Major comments of the reviewer

1) According to Figure 5, ozone measured observed at El Tololo increases substantially in the austral autumn (March-April) but shows some decreases in October. The largest ozone differences between El Nino and La Nina years also appear in March-April and September-October (Figure 11). However, the meteorological fields in Figure 3 are shown for DJF and JJA, which are not relevant to the key seasonal features shown in Figures 5 and 11.

Thanks for pointing this out. It is true that the climatology, as it is shown now, does not create any benefit for the reader. We therefore decided to show MAM and SON instead of DJF and MAM in Fig. 3 of the revised manuscript:

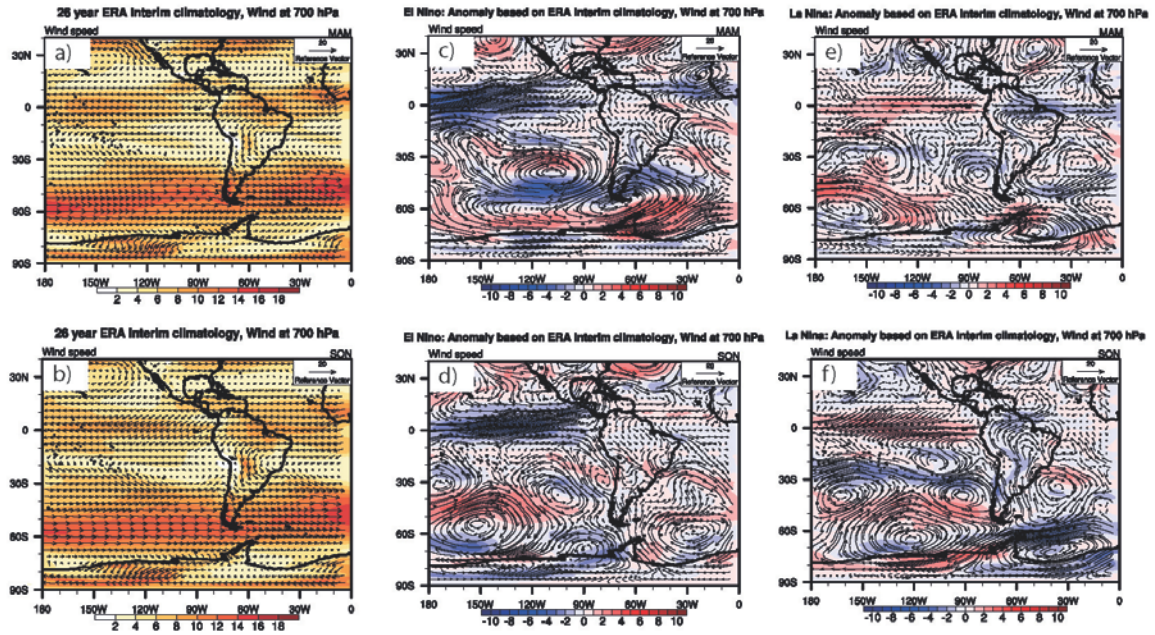

Fig. 1R2: ERA Interim wind climatology at 700 hPa (a, MAM and b, SON) and wind change in vector and strength during an exemplary El Niño event (1997-1998) (c, MAM and d, SON) and a La Niña event (1988-1989) (e, MAM and f, SON).

2) Figure 4b shows a time series for the deseasonalized monthly ozone data. Based on the plot, the authors noted in the text that it is not clear to see an ENSO signal. However, the influence of ENSO on ozone is known to have a strong seasonality (see also Figure 11). Why not also show a

time series of monthly ozone in March-April and September-October, respectively, and correlate the time series with the ENSO index?

Thanks for this valuable critique. It is true that the entire section 4.3 needs a thoughtful restructuring. Based on your suggestion, we tried to include a more in-depth discussion of the ENSO signal. We also included your idea to correlate the ozone time series with the MEI for the two periods (March-April and September-October) and have modified sect. 4.3 accordingly. We refer to "recommendations of the reviewer" for a more complete reply.

Should the slope shown on the top of Fig.4b be ppb/decade rather than ppb/y?

This is correct. We modified the slope legend.

It would be nice to also report the 95% confidence limits of the trends for annual mean and for each season.

We added, as also recommended by reviewer #1, the p-value and the confidence interval. Significant trends with 90% and 95% confidence are now labelled with * and **, respectively.

3) Figure 7 is very confusing. The figure caption notes that data at some sites are shifted by 182 days. Can you just separate the plot for the sites in the Northern Hemisphere versus the Southern Hemisphere without shifting the days and clearly label the latitude and longitude of each site?

Thanks for this comment. We agree that the shifting by half a year may be surprising to the reader, but makes the comparison of stations on the Northern hemisphere and the Southern hemisphere easier, as the seasons on both hemispheres will be aligned over another. In order to increase the readability, we modified the x-axis labels to name the season, and no more the day of year. We prefer this version rather than a separation of the plots, as this would result in a total of 4 plots, without significantly increasing the clarity. Moreover, we decided to add Mauna Loa (MLO) to the plot in order to include the station in the entire discussion.

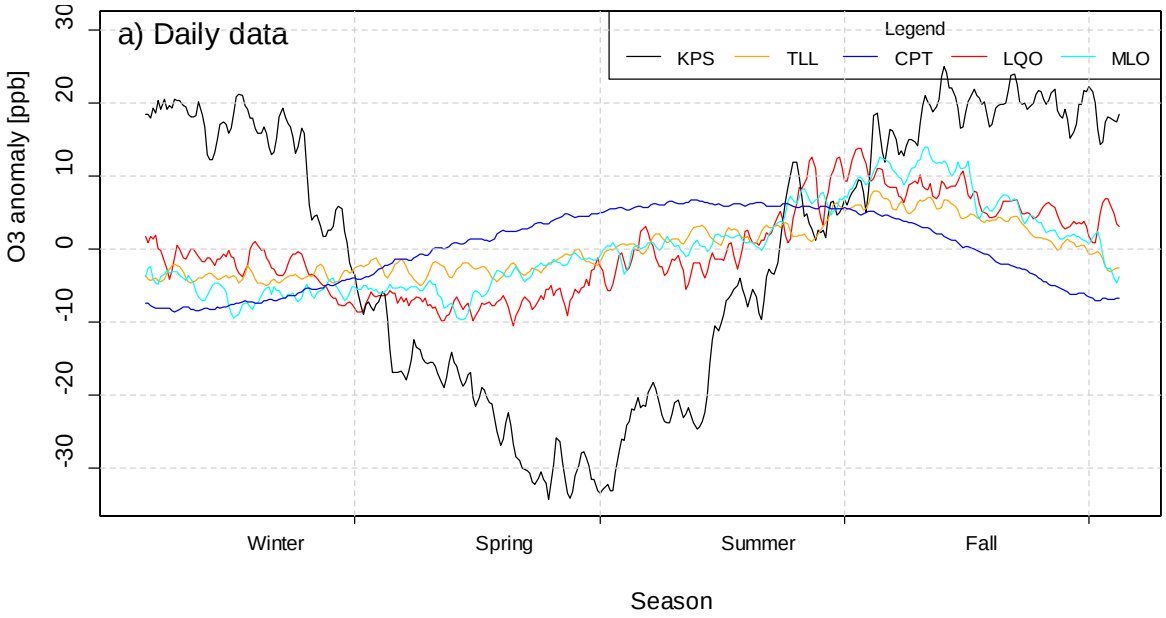

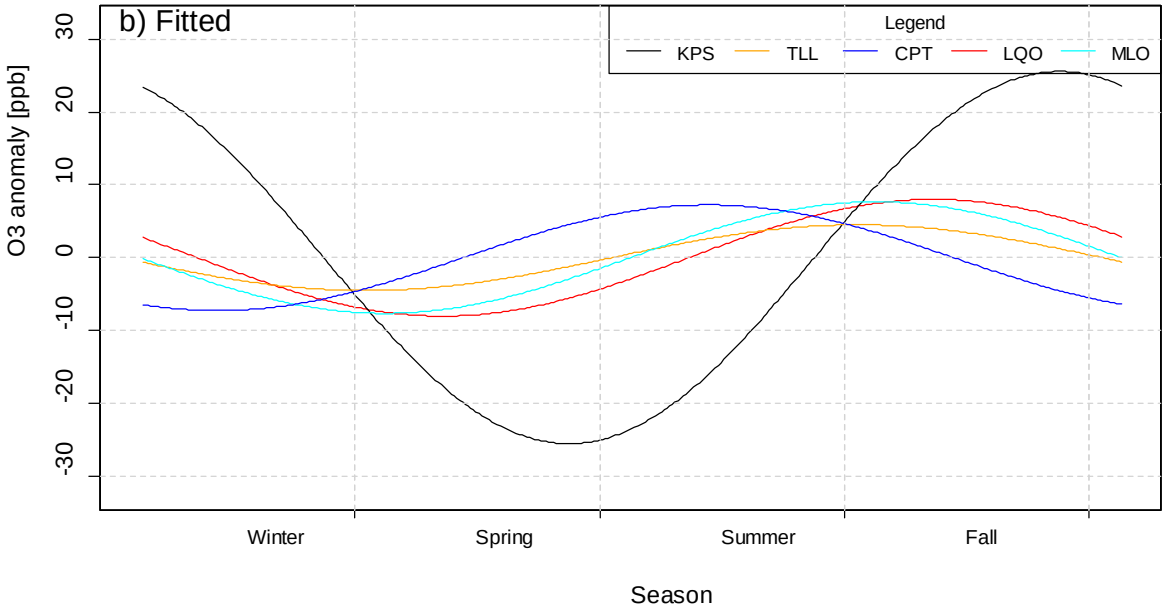

Another possible factor contributing to the seasonal cycle of ozone in the southern Hemisphere is biomass burning emissions, which the authors did not discuss at all. Please check the seasonal cycle of biomass burning activity in this region as reported in the published literature.

We are thankful that the reviewer pointed out this topic. It is however not entirely true that we did not discuss biomass burning at all. Several times, biomass burning is shortly discussed as a possible factor. Different studies have been cited concerning this topic. We can only repeat that regional biomass burning in the El Tololo region as well as over most of the Southern American continent is not a factor considering the footprint of air parcels travelling to El Tololo, and that influences from Africa or Australia are rather improbable (van der Werf et al., 2006). We nevertheless considered this point when editing section 3.4.

Recommendations of the reviewer

Similar to Mauna Loa Observatory in the Northern Hemisphere (Lin et al., 2014,Nature Geoscience), El Tololo (30S) is located in the subsiding branch of the Hadley Cell in the Southern Hemisphere. Ozone measured at Mauna Loa increases during boreal autumn (Sep-Oct) but shows no significant trend during boreal spring (March-April). Interestingly, ozone measured at El Tololo shows an increase during austral autumn (March-April) but no trend in austral spring (Sep-Oct). While the mechanisms controlling ozone trends at these two sites may be different, there are some similarities on their seasonal ozone trends. Thus, the referee strongly encourages the authors to carefully read Lin et al. (2014) and organize the analyses and associated discussions for El Tololo in a similar way to Mauna Loa. (*...following suggestion of restructuring the order of the figures...*)

We are grateful that the reviewer makes the link to Mauna Loa, another remote, high-altitude station located on the Northern Hemisphere. We did not discuss Mauna Loa due to different reasons:

- This paper was meant to present and discuss 20 years of ozone data from a southern hemispheric station, additionally to put it in context with other stations on both hemispheres, but not to compare it with one similar station from the northern hemisphere
- It is closer to upstream regions with large anthropogenic activities and thus, most likely stronger influenced by ozone precursors emissions
- Its location, more than 1000 km closer to the Equator, makes it difficult to classify it as a non-equatorial station

Yet, we realize that this was possibly a bit short-sighted. As noted above, we restructured section 4.3 entirely, also including a short discussion of similarities and differences to Mauna Loa, including the implicated MEI and QBO shear indexes. However, we tend to disagree that we should organize the analyses similar to the paper of Lin et al. (2014) due to following reasons:

- The manuscript intends to present a new station to the scientific community, first explaining its "special setting" compared to other GAW stations on the world
- We attempt to start from straightforward, rather simple-to-understand connections (like a simple trend analysis) and to later focus into deeper insights, analyzing annual cycles, comparing the station to other stations as well as ozone sonde measurements (in order to get a 3D-picture) and finally trying to link the recognitions with large-scale interactions like ENSO, or STE
- We followed the approaches of recent multi-station or multi-platform (in-situ, but also soundings, airborne observations, satellite products) O3 trend analysis (Logan et al., 2012;Parrish et al., 2013, 2012;Cooper et al., 2014) where changes in emissions and ozone photochemistry, changes in transport and pollution transport pathways, and potential of influence of climate change are investigated side-by-side

Please see also Fig.4 in the following manuscript. Their model also shows that free tropospheric ozone near El Tololo increases during austral autumn (MAM) but there is no significant trend in austral winter (JJA). I wonder if the observed ozone increase at El Tololo has something to do with the poleward shift of the subtropical jet stream in the Southern Hemisphere or changes in geopotential height patterns. The analysis suggested above will help in interpreting the cause of the seasonal trends.

We have attentively read the manuscript of Lin et al. (2016) and included a short discussion about the subtropical jet stream into section 4.3.

Reading the following articles might be useful for understanding the connections between ENSO and ozone variability. Introduction in the current manuscript focuses too much on precursor emission changes that are most relevant for polluted regions in the Northern Hemisphere. I think citing and discussing the findings from the following papers are more relevant to your analysis.

Thanks for these recommendations. They were of great help when restructuring section 4.3. We also included some ENSO-related introductions, citing the suggested publications and others:

Section 1: *Wang et al. (1998) and, more recently, Lin et al. (2015) state that at least some NH spring peaks originate from a combination of ozone-rich stratospheric influx (February-April) and formation by local ozone chemistry (April-June).*

Section 1: *At low latitudes, tropospheric ozone levels at remote sites are known to be sensitive to teleconnections like the El Niño/Southern Oscillation (ENSO). For example, Lin et al. (2014) analyzed the seasonal cycle of a long-term ozone dataset from Mauna Loa (Hawaii). There, long-term springtime ozone observations only marginally increased in the 2000s whereas fall ozone was observed to significantly augment in the 1990s. Lin et al. (2015) found the cause to be the ENSO, which, by altering SST, therefore convection and also large-scale atmospheric patterns, reduced (augmented) advection of air masses from Asia in spring (fall) during La Niña (El Niño) events. The ENSO-sensitive pattern does not limit itself to tropospheric ozone, but also to TCO, as has been shown in Ziemke et al. (2010), who retrieved an independent ENSO index based on TCO anomalies in the pacific region (Ozone ENSO index, OEI).*

Section 3.4: *There are several large-scale processes which potentially impact either short-term or long-term ozone variations at TLL. These factors include large-scale advection of air masses either via the subtropical jet or via potential vorticity cutoffs from the polar jet region, stratosphere-troposphere exchange of ozone-rich air from the stratosphere, as well as pattern changes in tropical up- or downwelling. The impact of these different elements vary not only over the course of a day (storm-scale) or of a year (seasonal cycles), but may also oscillate over timescales of two to seven years, following teleconnections and large-scale oscillations from features like the quasi biennial oscillation (QBO) or ENSO.*

All these influences are visible in the different ozone data products from TLL. We initially focus on the changes in the mean annual cycle of ozone over time and, based on this, elaborate further on the timing of the maximum and on the shape of the cycle. We conclude this section with a short overview of the observed short-term variations (week-scale) including a possible interpretation for those findings.

First, two mean seasonal cycles for two 5-year periods, one at the beginning of the measurements (1996-2000), and the other one in the recent past (2011-2015), were analyzed for potential differences. In Figure 5, the monthly means, with the upper 95th and the lower 5th percentiles including associated uncertainties are presented. Table 1 summarizes the findings in numbers. The two periods show a very similar annual cycle. However, there are subtle differences: Especially in austral fall (February-March), the 5^{th} percentile, mean, and the 95^{th} percentile increased remarkably from the first to the second period. Among the three curves, the 5^{th} percentile shows the most persistent increase from February up to June in the more recent period. For the other months of the year, changes are minor except for October, where 2011-15 shows slightly lower values of O_3. The annual cycle and some of the differences between the two periods are mainly driven by the annual cycle of ozone STE mass flux (see Fig. 5 and Fig. S9 in the supplementary material). However, the increase of ozone mole fractions from March to May cannot be explained by STE only, as at that time, ozone STE mass flux shows negative anomalies (Fig. S9). Here, three other factors like QBO or ENSO, change in large-scale dynamics and precursor species have to be taken into account. i): As Neu et al. (2014) showed, positive QBO shear and the multivariate ENSO index (MEI) lead to increased stratospheric air circulation, negative upper troposphere ozone anomalies (due to upwelling of relatively ozone-depleted air) and therefore to potentially decreased ozone-STE activity in the sub- and extratropics. Doherty et al. (2006) and Sekiya and Sudo (2012)) explained the decrease in total column ozone found in the eastern Pacific region during El Niño conditions with a decrease in NOx-production due to a decrease in lightning activity. The ozone anomalies at TLL and the MEI show significant correlations especially in September-October (cor=-0.78), and the annual cycles of ozone during El Niño years and La Niña years indeed show significantly different values especially in austral fall and spring (Fig. 11). During La Niña events, ozone levels reach higher values especially from September to November than during El Niño events. Fig. S10 in the supplementary material illustrates that the 1996-2000 period not only had a weak positive correlation (cor=0.28) of both (QBO shear/MEI) indexes, but also had one single strong El Niño event lasting nearly two years, possibly leading to a decreased ozone-STE burden in 1997/1998. The second, later period showed nearly no in-phase correlation of MEI and QBO shear index (cor=-0.04) and no significant El Niño event. ii): The subtropical jet has to be considered as contributing factor to the MAM anomaly in the 2011-2015 period. We assume that with the broadening of the Hadley Cell (HC, Choi et al., 2014;Nguyen et al., 2013), the extratropical jet, moving to higher latitudes, increasingly advected more polluted air from Southeast Asia, e.g. in form of Peroxyacetylenitrate (PAN, see also Jiang et al., 2016), during this period of the year, when biomass burning prevails (e.g. Streets et al., 2003). More work has to be done to confirm this theory, e.g. using satellite measurements, as this would go beyond the scope of this work. iii): An increase of biomass burning in Southeast Asia (e.g. Shi and Yamaguchi, 2014;Verma et al., 2015) and Australia (Cooper et al., 2014) with subsequent eastward transport of ozone precursors, could also explain the positive anomaly in MAM in the 2011-2015 period, as the as the Northward migration of the ITCZ during this time of the year starts to allow effects of NH emissions to be seen in the SH and prevailing westerly conditions (see

Fig. 3) exclude any sensitivity of ozone mole fractions at TLL to emissions on the South American continent. At most, the ozone increase may originate from regional pollution from the La Serena region, which – in fall – may get transported upwards due to the PBL height and occasional support by frontal systems. This latter assumption remains, however, hypothetical. A confirmation would require high-resolution numerical simulations to resolve the transport in the mountainous terrain of TLL. In summary, we conclude that the annual cycle is mostly STE-driven from June to January. From February to April however, the broadening of the HC with subsequent transport of pollutants from Southeast Asia, the contrast to El Niño dominated (1996-2000) versus average years (2011-2015) and the increase in precursor species in Southeast Asia are the best explanations for the positive ozone anomaly in the more recent period. From Table 1, we conclude furthermore that in general, differences between nighttime and daytime trends are very low which indicates that TLL is a very good background station with similar ozone levels under free tropospheric conditions and under planetary boundary layer (PBL) influence. Mean ozone mole fractions at TLL only vary between 32.5 and 31.0 ppb during day and night, while other stations located near greater cities (e.g. eastern US, Bloomer et al., 2010) report up to 50 ppb peak differences between nighttime and daytime. This finding is most probably attributed not only to the remote location, far away from pollutant sources, but also to the high altitude located above the PBL.

Regarding the 2-month lag between the recent maximum of STE ozone mass flux and the recent maximum of ozone mixing ratio in Figs. 7 vs. S9, we explain this delayed response of ozone to STE by following mechanisms: i) a certain amount of time is needed to equally distribute ozone stemming from STE in the lower troposphere (e.g. titration of NOx & HOx residing in the atmosphere) in order to reach chemical equilibrium and ii) deep convection underestimation as well as seasonal cycle uncertainties within the ERA Interim dataset (Škerlak et al., 2014) lead to doubts concerning the exact onset of ozone STE mass flux maximum around the cordillera.

What concerns the timing of the maximum, Fig. 8 shows a strong correlation (cor=0.89) between the mean annual cycle of STE trajectories (Škerlak, 2014) and of the ozone concentration. The two parameters show a strikingly similar pattern, indicating that STE may be a strong driver for O_3. Note that the mass flux illustrated in Fig. S9 shows a slightly earlier peak occurrence than the number of STE trajectories. Another indication for the coupling of O_3 concentration and STE is a coherent shift in the maximum of these quantities over the observation period towards an earlier occurrence in the year. This is illustrated in Fig. 10. For calculation, a 4-year sliding window of daily data was defined and run over all data between 1996 and 2015. Then, an empirical mode decomposition was done (Huang and Wu, 2008;Wu and Huang, 2009). Out of the Hilbert periodogram, the IMF resembling the most to an annual cycle is selected and the IMF-datapoints are extracted. The latter are averaged to get an average of IMF over the 4-year window. Finally, the day-of-year matching the maximum value of the IMF is extracted. For the ozone time series, a regression of -10 days per decade was calculated. For STT, an even larger trend of -11 or -21 days per decade was obtained for the maximum number of trajectories of stratospheric origin and for the mass flux into the PBL, respectively. Note that the regression is only poorly visible in Fig. 5, where data are aggregated in monthly bins and a comparison of 3 different percentiles of 5-year-monthly averages, instead of absolute maximal values, is shown.

This shift in the seasonal cycle to earlier times in the year has already been presented in other studies for other locations (Parrish et al., 2013;Lin et al., 2014). For instance, spring peaks are observed in the NH to

regress with a rate of 3 to 14 days per decade (Parrish et al., 2013). Parrish et al. (2013) also suggest that the relative contribution from the stratosphere may at least partly explain the shift in the annual cycle at high-altitude stations in the NH like Jungfraujoch, being located at 3580 meters asl. Yet, a conclusive explanation for this shift of the seasonal cycle remains missing. Schnell et al. (2016) recently suggested that future climate change will shift the maximum of the ozone seasonal cycle to earlier in the year, but they did not provide any clear explanation for this phenomenon.

Considering the short-term variations, it is known from previous studies that a (anti)correlation between ozone and relative humidity exists at TLL, but only in very specific cases. Gallardo et al. (2000) analyzing the first years of data collected at Tololo, found such an anticorrelation between ozone and water vapor in summer in connection with upslope transport of boundary layer air associated with a thermally driven circulation. Rondanelli et al. (2002) investigated the effect of troughs associated with a frontal zone passing over TLL, and could classify their observations in two categories: wet and dry events. During wet events, relatively humid air from the PBL is advected to TLL, and shortly after regression of relative humidity, ozone is rising rapidly. During dry events, ozone is rising, but relative humidity stays at normal, dry levels or drops even further. Carbon monoxide, a good PBL pollutant and hence an optimal tracer, has been measured in TLL since April 2013. Therefore, the dependence of CO and ozone was investigated. This analysis revealed a significant correlation (not shown) in rare, specific episodes, during which less pristine air from the PBL – originating from the La Serena, Valparaiso and Santiago regions – is reaching TLL. Those events were not always associated with low potential vorticity values (PV streamer, reconstructed from ERA Interim data, not shown) or frontal zones, but some of them were. This confirms the finding of Rutllant et al. (2013), who, during the VOCALS-REx-campaign, found a persistent, regular South-Westerly advection via thermals, being able to transport air masses in the afternoon from the marine region into the Andes which would allow inbound transport of slightly more polluted air masses to TLL. An in-depth analysis of CO-O_3-correlations over several years may be promising to provide more robust conclusions. However, the CO time series is still limited in time and an extended study would go beyond the scope of the paper.

References

Bloomer, B. J., Vinnikov, K. Y., and Dickerson, R. R.: Changes in seasonal and diurnal cycles of ozone and temperature in the eastern U.S, Atmospheric Environment, 44, 2543-2551, http://dx.doi.org/10.1016/j.atmosenv.2010.04.031, 2010.

Choi, J., Son, S.-W., Lu, J., and Min, S.-K.: Further observational evidence of Hadley cell widening in the Southern Hemisphere, Geophysical Research Letters, 41, 2590-2597, 10.1002/2014GL059426, 2014.

Cooper, O. R., Parrish, D. D., Ziemke, J., Balashov, N. V., Cupeiro, M., Galbally, I. E., Gilge, S., Horowitz, L., Jensen, N. R., Lamarque, J. F., Naik, V., Oltmans, S. J., Schwab, J., Shindell, D. T., Thompson, a. M., Thouret, V., Wang, Y., and Zbinden, R. M.: Global distribution and trends of tropospheric ozone: An observation-based review, Elementa: Science of the Anthropocene, 2, 000029-000029, 10.12952/journal.elementa.000029, 2014.

Doherty, R. M., Stevenson, D. S., Johnson, C. E., Collins, W. J., and Sanderson, M. G.: Tropospheric ozone and El Niño–Southern Oscillation: Influence of atmospheric dynamics, biomass burning emissions, and future climate change, Journal of Geophysical Research: Atmospheres, 111, n/a-n/a, 10.1029/2005JD006849, 2006.

Gallardo, L., Carrasco, J., and Olivares, G.: An analysis of ozone measurements at Cerro Tololo (30 degrees S, 70 degrees W, 2200 m.a.s.l.) in Chile, Tellus Series B-Chemical and Physical Meteorology, 52, 50-59, 10.1034/j.1600-0889.2000.00959.x, 2000.

Huang, N. E., and Wu, Z.: A review on Hilbert-Huang transform: Method and its applications to geophysical studies, Reviews of Geophysics, 46, n/a-n/a, 10.1029/2007RG000228, 2008.

Jiang, Z., Worden, J. R., Payne, V. H., Zhu, L., Fischer, E., Walker, T., and Jones, D. B. A.: Ozone export from East Asia: The role of PAN, Journal of Geophysical Research: Atmospheres, 121, 6555-6563, 10.1002/2016JD024952, 2016.

Lin, M., Horowitz, L. W., Oltmans, S. J., Fiore, A. M., and Fan, S.: Tropospheric ozone trends at Mauna Loa Observatory tied to decadal climate variability, Nature Geosci, 7, 136-143, 10.1038/ngeo2066

http://www.nature.com/ngeo/journal/v7/n2/abs/ngeo2066.html#supplementary-information, 2014.

Lin, M., Fiore, A. M., Horowitz, L. W., Langford, A. O., Oltmans, S. J., Tarasick, D., and Rieder, H. E.: Climate variability modulates western US ozone air quality in spring via deep stratospheric intrusions, Nature Communications, 6, 7105, 10.1038/ncomms8105

http://www.nature.com/articles/ncomms8105#supplementary-information, 2015.

Lin, M., Horowitz, L. W., Payton, R., Fiore, A. M., and Tonnesen, G.: US surface ozone trends and extremes from 1980-2014: Quantifying the roles of rising Asian emissions, domestic controls, wildfires, and climate, Atmos. Chem. Phys. Discuss., 2016, 1-56, 10.5194/acp-2016-1093, 2016.

Logan, J. a., Staehelin, J., Megretskaia, I. a., Cammas, J. P., Thouret, V., Claude, H., De Backer, H., Steinbacher, M., Scheel, H. E., Stbi, R., Frhlich, M., and Derwent, R.: Changes in ozone over Europe: Analysis of ozone measurements from sondes, regular aircraft (MOZAIC) and alpine surface sites, Journal of Geophysical Research: Atmospheres, 117, 1-23, 10.1029/2011JD016952, 2012.

Neu, J. L., Flury, T., Manney, G. L., Santee, M. L., Livesey, N. J., and Worden, J.: Tropospheric ozone variations governed by changes in stratospheric circulation, Nature Geosci, 7, 340-344, 10.1038/ngeo2138, 2014.

Nguyen, H., Evans, A., Lucas, C., Smith, I., and Timbal, B.: The Hadley Circulation in Reanalyses: Climatology, Variability, and Change, Journal of Climate, 26, 3357-3376, 10.1175/jcli-d-12-00224.1, 2013.

Parrish, D. D., Law, K. S., Staehelin, J., Derwent, R., Cooper, O. R., Tanimoto, H., Volz-Thomas, a., Gilge, S., Scheel, H. E., Steinbacher, M., and Chan, E.: Long-term changes in lower tropospheric baseline ozone concentrations at northern mid-latitudes, Atmospheric Chemistry and Physics, 12, 11485-11504, 10.5194/acp-12-11485-2012, 2012.

Parrish, D. D., Law, K. S., Staehelin, J., Derwent, R., Cooper, O. R., Tanimoto, H., Volz-Thomas, a., Gilge, S., Scheel, H. E., Steinbacher, M., and Chan, E.: Lower tropospheric ozone at northern midlatitudes: Changing seasonal cycle, Geophysical Research Letters, 40, 1631-1636, 10.1002/grl.50303, 2013.

Rondanelli, R., Gallardo, L., and Garreaud, R. D.: Rapid changes in ozone mixing ratios at Cerro Tololo (30°10′S, 70°48′W, 2200 m) in connection with cutoff lows and deep troughs, Journal of Geophysical Research: Atmospheres, 107, 1-15, 10.1029/2001JD001334, 2002.

Rutllant, J. A., Muñoz, R. C., and Garreaud, R. D.: Meteorological observations on the northern Chilean coast during VOCALS-REx, Atmos. Chem. Phys., 13, 3409-3422, 10.5194/acp-13-3409-2013, 2013.

Schnell, J. L., Prather, M. J., Josse, B., Naik, V., Horowitz, L. W., Zeng, G., Shindell, D. T., and Faluvegi, G.: Effect of climate change on surface ozone over North America, Europe, and East Asia, Geophysical Research Letters, n/a-n/a, 10.1002/2016GL068060, 2016.

Sekiya, T., and Sudo, K.: Role of meteorological variability in global tropospheric ozone during 1970–2008, Journal of Geophysical Research: Atmospheres, 117, n/a-n/a, 10.1029/2012JD018054, 2012.

Shi, Y., and Yamaguchi, Y.: A high-resolution and multi-year emissions inventory for biomass burning in Southeast Asia during 2001–2010, Atmospheric Environment, 98, 8-16, http://dx.doi.org/10.1016/j.atmosenv.2014.08.050, 2014.

Škerlak, B.: Climatology and process studies of tropopause folds , cross-tropopause exchange , and transport into the boundary layer, Dissertation, ETH ZURICH, 2014.

Škerlak, B., Sprenger, M., and Wernli, H.: A global climatology of stratosphere-troposphere exchange using the ERA-Interim data set from 1979 to 2011, Atmospheric Chemistry and Physics, 14, 913-937, 10.5194/acp-14-913-2014, 2014.

Streets, D. G., Yarber, K. F., Woo, J. H., and Carmichael, G. R.: Biomass burning in Asia: Annual and seasonal estimates and atmospheric emissions, Global Biogeochemical Cycles, 17, n/a-n/a, 10.1029/2003GB002040, 2003.

van der Werf, G. R., Randerson, J. T., Giglio, L., Collatz, G. J., Kasibhatla, P. S., and Arellano, a. F.: Interannual variability of global biomass burning emissions from 1997 to 2004, Atmospheric Chemistry and Physics Discussions, 6, 3175-3226, 10.5194/acpd-6-3175-2006, 2006.

Verma, S. K., Kawamura, K., Chen, J., Fu, P., and Zhu, C.: Thirteen years of observations on biomass burning organic tracers over Chichijima Island in the western North Pacific: An outflow region of Asian aerosols, Journal of Geophysical Research: Atmospheres, 120, 4155-4168, 10.1002/2014JD022224, 2015.

Wang, Y., Jacob, D. J., and Logan, J. A.: Global simulation of tropospheric O3-NO x -hydrocarbon chemistry: 3. Origin of tropospheric ozone and effects of nonmethane hydrocarbons, Journal of Geophysical Research: Atmospheres, 103, 10757-10767, 10.1029/98JD00156, 1998.

Wu, Z., and Huang, N. E.: Ensemble Empirical Mode Decomposition: A noise-assisted data analysis method, Advances in Adaptive Data Analysis, 01, 1-41, doi:10.1142/S1793536909000047, 2009.

Ziemke, J. R., Chandra, S., Oman, L. D., and Bhartia, P. K.: A new ENSO index derived from satellite measurements of column ozone, Atmos. Chem. Phys., 10, 3711-3721, 10.5194/acp-10-3711-2010, 2010.

Surface ozone in the southern hemisphere: 20 years of data from a site with a unique setting in El Tololo, Chile, 30°N, 71°W, 2200 m asl

Julien G. Anet[1,2], Martin Steinbacher[1], Laura Gallardo[3,4], Patricio A. Velásquez Álvarez[5,6], Lukas Emmenegger[1], Brigitte Buchmann[1]

[1]Laboratory for Air Pollution / Environmental Technology, Swiss Federal Laboratories for Materials Science and Technology, Duebendorf, Switzerland
[2] WSL Institute for Snow and Avalanche Research SLF, Davos, Switzerland
[3]Departamento de Geofísica de la Universidad de Chile, Blanco Encalada 2002, piso 4, Santiago, Chile
[4]Center for Climate and Resilience Research (CR2), Blanco Encalada 2002, Santiago, Chile
[5]Dirección Meteorológica de Chile, Av. Portales 3450, Estación Central, Santiago, Chile
[6]Climate and Environmental Physics, Physics Institute, University of Bern, Bern, Switzerland

Correspondence to: Julien G. Anet (julien.anet@empaslf.ch), Martin Steinbacher (martin.steinbacher@empa.ch)

Abstract. The knowledge of surface ozone mole fractions and their global distribution is of utmost importance due to the impact of ozone on human health and ecosystems, and the central role of ozone in controlling the oxidation capacity of the troposphere. The availability of long-term ozone records is far better in the northern than in the southern hemisphere, and recent analyses of the seven accessible records in the southern hemisphere have shown inconclusive trends. Since late 1995, surface ozone is measured in-situ at "El Tololo", a high-altitude (2200 m asl) and pristine station in Chile (30°S, 71°W). The dataset has been recently fully quality-controlled and reprocessed. This study presents the observed ozone trends and annual cycles and identifies key processes driving these patterns. From 1995 to 2010, an overall positive trend of ~0.7 ppb/decade is found. Strongest trends per season are observed in March and April. Highest mole fractions are observed in late spring (October) and show a strong correlation with ozone transported from the stratosphere down into the troposphere, as simulated with a model. Over the 20 years of observations, the springtime ozone maximum has shifted to earlier times in the year which, again, is strongly correlated with a temporal shift in the occurrence of the maximum of simulated stratospheric ozone transport at the site. We conclude that background ozone at El Tololo is mainly driven by stratospheric intrusions rather than photochemical production from anthropogenic and biogenic precursors. The major footprint of the sampled air masses is located over the Pacific Ocean. Therefore, due to the negligible influence of local processes, the ozone record also allows studying the influence of El Niño and La Niña episodes on background ozone levels in South America. In agreement with previous studies, we find that during La Niña conditions, ozone mole fractions reach higher levels than during El Niño conditions.

1 Introduction

Tropospheric ozone (O_3) is a key atmospheric compound that plays an important role in many respects: It acts as a greenhouse gas, which is contributing to radiative forcing of up to 21% relative to the radiative forcing induced by CO_2 (Myhre et al., 2013). Ozone has adverse effects on crop yields and on human health, being an irritating agent and triggering asthma and cardiovascular diseases (Reich and Amundson, 1985;Brook, 2002;Fiscus et al., 2005). Ozone is also a major source of hydroxyradicals and, thereby, influences the oxidative capacity of the atmosphere (Crutzen, 1971;Staehelin et al., 2001).

Various processes determine the amount of ozone in the troposphere: ozone is naturally produced by oxidation of methane, by reaction of oxygen with lightning-induced NO-production, as well as by photochemical formation in the presence of volatile organic compounds (VOCs), nitrogen oxides (NOx) and sunlight (Crutzen, 1971;Crutzen, 1973;Crutzen and Zimmermann, 1991;Winer et al., 1992;Derwent et al., 1998). Thus, changes in ozone precursor emissions – which are partly due to anthropogenic activities – considerably influence the tropospheric ozone burden. However, a straightforward attribution of emission changes to ozone trends is challenging due to the highly non-linear photochemistry, different (VOC- and NOx-limited) ozone production regimes and also photochemical loss processes (Crutzen, 1971;Sillman and He, 2002). A significant part of tropospheric ozone origins from stratosphere-troposphere-transport (STT), also known as stratosphere-troposphere-exchange (STE), happening e.g. in tropopause folds (Holton et al., 1995;Škerlak, 2014;Škerlak et al., 2014;Lefohn and Cooper, 2015). The STE is not evenly distributed over the globe and hotspots of transport of stratospheric ozone into the planetary boundary layer exist in the region of the Rocky Mountains, Tibetan Plateau, Andes (around 30°S), storm tracks, and Indian Ocean (Škerlak et al., 2014). Recent modelling studies postulate that the contribution from STE to the tropospheric ozone burden may be as high as 23 % of the net photochemical production (Stevenson et al., 2006;Sudo and Akimoto, 2007). This contribution may change in the future due to climate change and could lead to more than 20% STT increase (Collins et al., 2003;Hegglin and Shepherd, 2009;Neu et al., 2014).

Ozone sinks include catalytic destruction involving HO_2 and photolytic destruction; O_3 can also be removed from the atmosphere by dry deposition, wet scavenging and uptake by vegetation (Galbally, 1968;Stevenson et al., 2006).

The first ozone observations in the atmosphere were performed in the nineteenth century in Montsouris/Paris (Volz and Kley, 1988). However, regular and geographically distributed measurements have become more established only in the second half of the 20th century. Nowadays, surface ozone observations are widespread and data are available from various data repositories such as the World Data Centre for Greenhouse Gases (WDCGG) of the Global Atmospheric Watch (GAW) programme of WMO, or from regional environmental agencies like the European Environment Agency (AirBase), the US Environmental Protection Agency (CASTNET, AQS) or the Acid Deposition Monitoring Network in East Asia (EANET). ~~However~~Currently, observations in the southern hemisphere in general, and in South America in particular, are very sparse (Sofen et al., 2016a;Sofen et al., 2016b).

Following Cooper et al. (2014), Oltmans et al. (2013) and Parrish et al. (2012), emissions of anthropogenic volatile organic compound and hydrocarbon emissions have led to a strong rise of ozone production in the last century. In fact, ozone has been generally increasing by up to 3 or 7 ppb/decade in the southern (SH) and northern (NH) hemisphere, respectively, averaged over different time spans (all between 1971 to 2011 and at least averaged over 10 years, see e.g. Table 1 of Cooper et al. (2014)). Thorough research has been undertaken to explain the difference in the trends between the two hemispheres. A possible explanation of the more pronounced trend in the NH is i) higher precursor emissions than in the SH, and ii) relatively short lifetime of ozone and subsequent lack of transport into the SH. Moreover, trends in the NH are very different from location to location. Recent work raised the attention to the flattening of the positive trend in NH tropospheric ozone at certain sites, especially at those located in Europe or eastern Northern America (Cooper et al., 2014). At most stations, this finding can be explained by decreasing nitrogen oxides (NO_x = NO+NO_2) emissions in the developed western countries. Such a levelling off is currently not observed in the western Unite~~d~~ds States as NO_x sources in upstream regions such as eastern Asia are still significantly increasing (Cooper et al., 2012). In contrast, the few SH ozone monitoring stations only partly recorded a flattening of the trend (Cooper et al., 2014). These ozone time series either show increasing positive trends (Oltmans et al., 2013;Thompson et al., 2014), or no significant change at all (Oltmans et al., 2013;Cooper et al., 2014). A world-wide map of ozone trends interpolated from the existing surface ozone measurement stations is not yet available. Wespes et al. (2016) recently tried to map ozone mixing ratio trends in the lower troposphere by using remote sensing satellite data from 2008-2013. They showed that ozone mixing ratios in the lower troposphere were generally decreasing all over the southern hemisphere and in most parts of the northern hemisphere during this period. However, this trend cannot be generalized as polluted areas of the world still show significant positive ozone trends.

Tropospheric ozone records often show a pronounced seasonal cycle. While in polluted areas, a strong photochemically driven summer peak is observed, a spring peak with stratospheric influence dominates in most continental pristine regions (Wang et al., 1998a;Wang et al., 1998b;Monks, 2000). Stations in the marine boundary layer in the SH such as Cape Grim, Australia, rarely reveal a distinct spring peak, but rather show a summer peak due to HO_2 photochemistry (Ayers et al., 1992;Monks, 2000). Measurements in the SH free troposphere (e.g. La Quiaca, Argentina, 3459 m asl) show a spring maximum (Barlasina et al., 2013), similar to the NH ozone time series from unpolluted stations. These findings were more broadly confirmed by Cooper et al. (2014), who, using satellite-measured total column ozone datasets, classified the onsets of the Total Column Ozone (TCO) maxima globally. In general, spring TCO maxima are found rather on the SH, while summer TCO maxima are prominent in the NH. This latter work is in contrast to the ~~finding~~ results of Monks (2000), who concluded that the spring phenomenon is primarily a NH feature. Wang et al. (1998a) and, more recently, Lin et al. (2015) state that ~~this~~ at least some NH spring peaks originate~~s~~ from a combination of ozone-rich stratospheric influx (February-April) and formation by local ozone chemistry (April-June).~~–~~A recent analysis of the ozone seasonal cycle at northern midlatitudes revealed a shift of these ozone spring peak concentrations backwards by 3 to 6 days per decade (Parrish et al., 2013). They conclude that this feature may be explained by changes in atmospheric dynamics, possibly combined with variations in the geographical distribution of the precursor emissions.

At low latitudes, tropospheric ozone levels at remote sites are known to be sensitive to teleconnections like the El Niño/Southern Oscillation (ENSO). For example, Lin et al. (2014) analyzed the seasonal cycle of a long-term ozone dataset from Mauna Loa (Hawaii). There, long-term springtime ozone observations only marginally increased in the 2000s whereas fall ozone was observed to significantly augment in the 1990s. Lin et al. (2015) found the cause to be the ENSO, which, by altering SST, therefore convection and also large-scale atmospheric patterns, reduced (augmented) advection of air masses from Asia in spring (fall) during La Niña (El Niño) events. The ENSO-sensitive pattern does not limit itself to tropospheric ozone, but also to TCO, as has been shown in Ziemke et al. (2010), who retrieved an independent ENSO index based on TCO anomalies in the pacific region (Ozone ENSO index, OEI).

The GAW ozone network has a satisfactory station coverage over the NH. This is not the case for the SH, where the network is very sparse and additional surface ozone time series are needed to understand the global picture of ozone dynamics. This paper describes a recently quality controlled 20-year surface ozone dataset from "El Tololo", a mountain site in Chile, South America, where ozone and a standard set of meteorological variables have been measured since 1995. Recently, the station has been equipped with a new ozone monitor and a CO/CO2/CH4 analyzer by Empa (Swiss Federal Laboratories for Materials Science and Technology).

El Tololo is currently the only GAW station in the SH above the marine boundary layer regularly submitting tropospheric ozone data to WDCGG. Therefore, the station provides highly valuable information on the ozone distribution in the unpolluted atmosphere. Gallardo et al. (2000) and Rondanelli et al. (2002) published analyses of the early phase of the ozone record, pointing at particular characteristics of the ozone time series in connection with large-scale Hadley circulation, cut-off lows and deep troughs, or related to transport from the boundary layer.

The main objective of this study is to characterize the complete time series of this station which is likely representative of a large domain of the background SH and to provide insight into the key processes driving the observed variability and trends. Section two gives an overview of the measurement station, and the instrumentation. In section three, the data series are presented and interpreted. Finally, we present our conclusions in the last section.

2 Station characterization

2.1 Location

The atmospheric monitoring station "El Tololo" (TLL) is located in the Coquimbo-region at 2200 m asl, 30°.17S, 70°.79W, 400 km north of Santiago de Chile, around 90 meters below the top of the mountain "Cerro Tololo". At Cerro Tololo, astronomical telescopes and instruments are operated as the Cerro Tololo Inter-American Observatory (CTIO) which belongs to the US National Optical Astronomy Observatory (NOAO). The Chilean Meteorological Service (Dirección Meteorológica de Chile, DMC) runs the El Tololo station on the CTIO area. The distance from El Tololo to the next bigger cities is 50 km to the NW (La Serena/Coquimbo) with smaller towns nearby (Vicuña 20 km NE, Paiguano 30 km NE,

Andacollo 30 km SW, Ovalle 60 km SW, see Fig. 1). Fifteen kilometers North of El Tololo, the Elqui-Valley, which is dominated by agricultural activity, is located in a W-E elongation. The population density of this region is low, accounting 17 inhabitants per km^2.

2.2 Climatology

Climate at TLL is classified as cool and arid. Between 1995 and 2015, the average temperature was 13.4°C (see Fig. S3 in the supplementary material) and in most years, less than 70 mm of rainfall was registered which can be classified as a "desert climate" (BWk) following Köppen climate classification of Geiger (1961) and Kottek et al. (2006). The wind measured at TLL mostly blows from the SSW sector during the summer months (December, January, and February, DJF) and from the NNE sector during the remaining time of the year (see Fig. S4). However, the wind direction data does not necessarily represent the free atmosphere, as the local topography at the station partially obstructs advection from the NW to N sectors. Moreover, turbulent eddies downwind of the mountain top influence the measured wind direction. Kalthoff et al. (2002) described the mesoscale wind regimes affecting the area.

In order to identify the main origin of the air masses arriving at TLL, backward trajectory simulations from the FLEXTRA model (e.g. Stohl et al., 1995), calculated at Empa, were used. The model uses wind fields from the European Centre for Medium-Range Weather Forecasts (ECMWF), and subsequent analysis locates the source of the trajectories in the Northwest to South sector with some rare events from the North and Southeast (see Fig. 2). The influence of air parcels from the northeastern parts of South America is minor since the Andes are efficiently blocking any advection of air masses from this direction. Therefore, local pollution events from the greater Santiago de Chile region are more relevant than large-scale pollution events originating, e.g., from biomass burning in the Amazon region. 71% of the 10-day-trajectories start at an altitude between 0 and 5000 meters, and 10 % of the 10-day-trajectories originate from altitudes higher than 8000 meters (see Fig. S5 in the supplementary material). The origins of the trajectories follow clearly distinguishable seasonal patterns: during the summer months (DJF), most trajectories originate from south of the station and from the lower troposphere. During the winter months (JJA), more trajectories start north of the station, as the south-eastern pacific high shifts to more northern latitudes at that time of the year (e.g. Rahn and Garreaud, 2014). This also explains why trajectories from the upper troposphere are more frequent in JJA compared to DJF (+50%), following increased subsidence. The mean air trajectory length is highest during spring time (SON) and lowest during fall (MAM, see Fig. S6).

Being located in the subtropics, TLL is rarely affected by frontal or cyclonic systems. Nevertheless, during spring and summer time (SON, DJF), cut-off lows and troughs from higher latitude may reach subtropical regions, thus influencing the large-scale advection patterns at TLL (Rondanelli et al., 2002) on short time scales. This leads both to advection of polar air masses as well as upward-transport of marine boundary layer air potentially polluted by human activities in the nearby cities, possibly influencing the chemical composition of the air at TLL.

Apart from meteorological frontal systems, climatological patterns like the ~~El Niño Southern Oscillation (~~ENSO~~)~~ do influence the large-scale origin of air masses arriving at TLL. In Fig. 3, the wind climatology and the change in the wind

field during an exemplary strong El Niño (1997-1998) and La Niña (1988-1989) event are shown for austral spring and austral fall (ERA Interim, 700 hPa wind, climatology from 1979-2015, see Methods section for details).

The subtropical Pacific high determines subsidence in the Tololo area year-around interrupted occasionally by passing fronts or cut-off lows (Fuenzalida et al., 2005). It also drives a low-level jet (LLJ) along the west coast of South America, which peaks in intensity in spring (Garreaud and Muñoz, 2005;Muñoz and Garreaud, 2005). During El Niño (La Niña) years, the Pacific high becomes weaker (stronger), which leads to negative (positive) anomalies in subsidence and coastal southerly winds.

As mentioned earlier, ozone transport due to STE is an important factor of the tropospheric O_3 burden particularly in the remote SH. The ERA interim climatology shows a "hotspot" of downward transport of stratospheric, ozone-rich air masses above TLL (cf Fig. 2 in Škerlak et al., 2014), especially during austral spring and summer. This can most probably only be explained by gravity wave triggering when air parcels originating from the southern pacific region suddenly encounter a strong change in orographic height (Andean barrier, up to 6000 m asl). Moreover, the weakening of the subtropical jetstream in DJF favors additional wave breaking, triggering downward transport of ozone through tropopause folds. This potentially leads to a higher burden of tropospheric ozone in DJF. We will discuss this subject more thoroughly later in this work.

3 Data and Methods

3.1 Ozone data at El Tololo

In 1995, TLL has been equipped with an ozone photometer and a set of meteorological sensors. Ozone at TLL is measured by UV absorption with a Thermo Environmental Instruments Inc. TECO 49-003 analyzer. The station is equipped with an external ozonator which allows producing defined levels of ozone to conduct performance checks. Measurements are done continuously and data are recorded on a Campbell Scientific 21X data logger as 15-minute averages. Zero and span checks on multiple levels are done twice weekly and once monthly, respectively, to keep track of the background signal and the instrument response. Regularly, the operator visually inspects the recorded data for obvious anomalies.

The TECO 49-003 analyzer measures the UV light absorption in the Hartley band (220-310 nm) where ozone is a strong absorber. The optical bench is a dual cell device which is connected to a mercury lamp (245 nm) as light source. Alternately, one cell is flushed with ozone-free air while the other is simultaneously flushed with sample air. This allows a correction for changes in light intensity and potential interfering species. The TECO 49-003 has a sensitivity of ±1 ppb and a precision of 2 ppb. The response time is on the order of 20 seconds to reach 95% of the new signal (TEI, 1992). In September 2010, instrument performance of the analyzer was assessed during the SMN/WMO/GAW - 4th Tropospheric Ozone Analyzer Intercomparison at the Servicio Meteorológico Nacional, Observatorio Central de Buenos Aires, Buenos Aires, Argentina. The instrument passed all checks and a comparison with an ozone traveling standard of the World Calibration Centre for

Surface Ozone (WCC-Empa) confirmed the validity of the instrument calibration (see WCC report at http://empa.ch/documents/56101/250799/2010_BsAs_RCC-O3.pdf).

In early 2013, the station has been equipped with an additional instrument measuring greenhouse gases (Picarro Inc. G2301 CRDS for CO_2/CH_4/CO and H_2O analysis) and a refurbished ozone photometer (Thermo Scientific, TE49c) using the same measurement principle as the TECO 49, as the latter is reaching its end of life. The two independent ozone time series agree well. A small systematic offset has been observed which is most likely due to different inlet heights above ground for the two measurement systems. A short overview comparing the overlapping measurements of the two devices is given in the supplementary material (section S1, Fig. S1). Figure S7 shows the time series of meteorological parameters.

3.2 Ozone data used in this study

In-situ ozone data from other surface stations in the GAW network (K-Puszta (Hungary), Ushuaia (Argentina), Cape Point (South Africa), Cape Grim (Australia), and La Quiaca (Argentina), see https://gawsis.meteoswiss.ch for more details) were downloaded from the World Data Centre for Greenhouse Gases (WDCGG; http://ds.data.jma.go.jp/gmd/wdcgg/) and are used for comparison purposes.

In addition to the surface ozone measurements, ozone sondes are recording valuable information about the vertical ozone distribution in the atmosphere e.g. within the SHADOZ project since 1998 (Thompson et al., 2007). Frequent data is available from Ascension Island (United Kingdom), Suva (Fiji), Watukosek (Java), Natal (Brazil), La Réunion (France), Pago Pago (American Samoa), San Cristobal (Ecuador), and Irene (South Africa), where sondes have been launched every 2 to 6 days. Additionally, ozone soundings from Easter Island (Rapa Nui, Chile) have been kindly provided by the DMC (pers. comm. P. Velázquez) as the long term data were not available from any data centre yet. The ozone sondes are all equipped with an Electrochemical Concentration Cell (ECC). According to Thompson (2003) the agreement between the sonde and the ground-based measurements lies around 2-7%.

Model data from two sources is used in this work to study the atmospheric large-scale influences on the local measurements at TLL: i) a Stratosphere-Troposphere ~~Transport~~ Exchange (STE) climatology from Škerlak et al. (2014) and ii) wind field climatologies from the ERA-Interim reanalysis. The STE climatology allows identifying the footprint of a potential ozone contribution from the stratosphere, while the ERA-Interim reanalysis is used to help understanding the effect of climatic variability associated, for example, with ENSO.

3.3 Methods

Prior to the long-term trend analysis, data are rigorously screened to eliminate all data potentially influenced by local pollution. In a first step, values above 55 ppb or below 10 ppb are flagged and visually inspected for outliers, as those data points mostly arise from zero/span checks or local influences (Fig. S2a in the supplementary material). In a second step, a further filtering is applied inspired by the well-established approach from Thoning et al. (1989) applied to the long-term CO_2 record at Mauna Loa, Hawaii. Adopting their method to ozone and to the conditions at El Tololo, data points with ozone

mole fractions experiencing a change of more than 4 ppb from one hour to the next are excluded (Fig. S2b). This value of 4 ppb has been defined as such to avoid too many false positives or negatives during the automatic filtering process, in order to minimize the workload during the manual dataset review process. In a third step, a polynomial fit is applied to the nocturnal data (23:00-06:00 LT) and data points exceeding twice the standard deviation of all data points of the nocturnal fit computed over one night are excluded (Fig. S2c & d). An example of the effects of this filtering can be seen in the supplementary material, section S2. A final visual inspection is performed, in order to exclude any periods of sampling problems or local pollution events referenced in the station log books (see Table S1). As well, correction of "false negatives" flagged by the automatic filtering routine can be recovered. Only then, the 15-minute ambient air data is averaged to hourly data, hourly averages to daily data, and daily averages to monthly data. The filtering excludes approximately 4.9% of the available data indicating the pristine setting of the sampling site with hardly any influence from local pollution sources from the premises' infrastructure.

Trends are computed from filtered, de-seasonalised monthly averages. Deseasonalization is done using an additive model (Kendall and Stuart, 1983), separating the seasonal component and the trend from the time series. Significance is estimated by means of a two-sided Student t-Test at the 5% significance level except where explicitly noted. In order to make the analysis more robust, all-time (24 h), nighttime (22-04 LT) and daytime (11-17 LT) data is analyzed separately. To discern changes in the diurnal and annual cycle, seasonal and monthly means based on hourly data of two periods (1996-2000 and 2011-2015) are computed. Correlation tests are assessed with the Pearson's product moment correlation coefficient, which is following a t-distribution.

To discern changes in the annual cycle, daily data have also been investigated. The Huang-Hilbert transform technique was selected to decompose those daily data into intrinsic mode functions (IMF) with the use of ensemble empirical mode decomposition (EEMD, Huang and Wu, 2008;Wu and Huang, 2009). The EEMD allows decomposing the time series into a residual trend and various oscillating signals representative of variations at seasonal, synoptic and other time scales. EEMD turned out to be particularly powerful for this time series analysis as it succeeds to mimic the asymmetric seasonal cycle peaking in October (see later) which is rather hard to match with sine-curve fitting.

Datasets of daily averages from the other GAW stations do not undergo the filtering process. However, in order to distinguish more easily the time at which seasonal maximum ozone mole fractions occur, a running mean with a window of 4 days is applied to the data, including those of TLL.

Ozone sounding data (see section 3.2) was cumulated per station in order to get annual cycles as follows: For each station, all soundings with valid data were temporally aligned, in order to reach data densities of as many days per year as possible, thus creating a small climatology. Multiple values for the same day of the year were averaged. Stations with less than 70% data coverage in a given year were rejected. Similarly to the surface stations, the annual cycle is smoothed with a running mean (width of filter: soundings with visually homogeneous, regular seasonal cycle=10 days; soundings with visually irregular seasonal cycles [Macquarie island, Marambio, and Ushuaia]=20 days) at pressure levels of 1000 hPa, 900 hPa, 800 hPa, 700 hPa, 600 hPa and 500 hPa in order to compute the timing of the seasonal ozone maximum for several altitudes.

The dataset used for large-scale stratosphere-to-troposphere ozone transport studies (Škerlak et al., 2014) is based on the ERA-Interim reanalysis (ERAI) data from ECMWF (Simmons et al., 2007). Driven by the wind field of ERAI, Škerlak et al. (2014) calculated ~~are calculated~~ kinematic trajectories using an 3-steps iterative Eulerian integration scheme (Sprenger and Wernli, 2015). Trajectories are started on a dense global grid and calculated for 24 hours, where only the ones crossing the tropopause are flagged. These flagged trajectories are extended 4 days backward and forward, and those with a residence time in the troposphere shorter than 48 h are excluded from the climatology. Škerlak et al. (2014) estimated a transport of 6.52 * 10^11 kg of ozone per trajectory (Δm_{O_3}) which is given by the size of the model grid cell. The mass flux (ΔMF_{O3}) is then a ~~simple~~ multiplication of the number of trajectories (n) per unit of time (t) times the mass of ozone transported downwards through a certain model level surface (Δm_{O_3}):

$$\Delta MF_{O_3} \approx n * t * \Delta m_{O_3}$$

For example, mass fluxes around TLL (see Fig. S8 in the supplementary material) amount to 8-10 kg/(km^2 s); for comparison, the half-morning production of ozone over the whole city of Santiago de Chile (641 km^2) on a summer day amounts to around 6680 kg/3 hours (Elshorbany et al., 2009).

4 Results and Discussion

The complete available ozone dataset at TLL from 1996 to 2015 is shown in Fig. 4a. There are only a few extended data gaps, which are all documented in the station log book (see supplementary material, Table S1). The overall data availability is 87%.

4.1 Long-term ~~T~~trend analysis

Time series of the filtered deseasonalized monthly means is shown in Fig. 4b. A highly significant increase of 0.66 ppb/decade is found for the entire period from 1996-2015 (p-value 0.0008). The variability of the filtered deseasonalized monthly means is within ±8 ppb.

The deseasonalized ozone time series can be further decomposed using the Huang-Hilbert transform technique. By analyzing the residual, a flattening and a reversal of the trend are observed since 2008 and 2010, respectively (Fig. 4c). Up to September 2010, the EEMD calculation reveals a positive linear trend of 0.67 ppb/decade which is in accord to the linear fit. The EEMD calculation reverses after September 2010 resulting in a negative trend of -0.41 ppb/decade.

Long-term trends similar to TLL can also be found at other stations in both the SH and the NH. Perennial trend analysis can be found in the literature e.g. for Cape Point, Mace Head, Cape Grim, Mauna Loa and western US regions (e.g. Yellowstone NP, Lassen, and others), and most of them show a distinct increase in ozone mixing ratios up to the millennial years - though mostly larger than at TLL, - before showing signs of levelling off (GAW, 2013;Carslaw, 2005;Derwent et al., 2013;Derwent et al., 2007;Oltmans et al., 2013;Cooper et al., 2014;Baylon et al., 2015;Lin et al., 2014). This phenomenon is particularly pronounced at certain NH stations in Europe and in the western US, as shown in Cooper et al. (2014): global ozone

concentrations which have been rising for more than 20 years tend to level off and even reverse quite significantly in those regions since the millennial change. This is primarily due to large scale changes in NOx and VOC emissions. In contrast, some western US stations still show signs of growing ozone concentrations, as they are downwind of pollutants from eastern Asia. Those stations, including Mauna Loa (Hawaii), sampling air with origin over the Pacific Ocean, may be partly comparable with the TLL station which is as well sampling air from oceanic origin, although the emissions of pollutants upwind of the western US coast are by far much higher than the emissions at similar longitudes from southern hemispheric regions (e.g. Janssens-Maenhout et al., 2015). NH emissions are moreover prevalent over the whole year (industrial, coal mining and energy production being the greatest sources), compared to those of the SH which are rather to be classified as seasonal peaks from biomass burning, originating in Southeast Asia. Considering however the influence of ENSO on the ozone time series (see 4.3), we conclude that air at TLL is certainly influenced at least by a fraction by air masses originating in Southeast Asia/Australia.

~~The reversal around 2010 is about in agreement with Oltmans et al. (2013) who find indications of a declining trend in the SH at one station (Cape Grim, Australia) at least, taking into account data up to 2010. A quick analysis of the trends of deseasonalized monthly averages of the stations Cape Point (South Africa) and Cape Grim (Australia) reveal a flattening (Cape Grim) respectively a reversal of the trend (Cape Point) from 2011 on, which is qualitatively in agreement with our findings for El Tololo (not shown). This phenomenon is even more pronounced in the NH, as shown in Cooper et al. (2014): global ozone concentrations which have been rising for more than 20 years tend to level off especially in the eastern parts of the US and in Europe. This is primarily due to large scale changes in NO_x and VOC emissions.~~

~~Changes in regular patterns over time provide useful information to understand the underlying drivers and processes. Therefore, the mean seasonal cycles for two 5 year periods, one at the beginning of the measurements (1996 2000), and the other one in the recent past (2011 2015), were analyzed for potential differences. In Figure 5, the monthly means, with the upper 95th and the lower 5th percentiles including associated uncertainties are presented.~~

~~The two periods show a very similar annual cycle. However, there are subtle differences: Especially in austral fall (February-March), the 5th percentile, mean, and the 95th percentile increased remarkably from the first to the second period. Among the three curves, the 5th percentile shows the most persistent positive deviations from February up to June in the more recent period. During the remaining of the year, changes are minor except for October, where 2011-15 shows slightly lower values of O_3. The annual cycle and some of the changes over time are partly driven by the annual cycle of ozone STE mass flux (see Fig. S9 in the supplementary material). Especially the shift of maximum from October to August (see later, Fig. 10) is represented by a drop of ozone mole fractions in October in Fig. 5. This can be explained by the modelled decrease of ozone mass flux in September and October and, conversely, increase of the mass flux in August (Fig. S9). However, the increase of ozone mole fractions from March to May cannot be explained by STE only, as at that time, ozone STE mass flux shows negative anomalies (Fig. S9).~~

~~The attentive reader may have realized that the maximum of STE mass flux (Fig. S9) and the maximum of ozone mixing ration (Fig. 5) are shifted by two months. We explain this delayed response of ozone mole fractions to STE by following~~

mechanisms: i) a certain amount of time is needed to equally distribute ozone stemming from STE in the lower troposphere (e.g. titration of NOx & HOx residing in the atmosphere) in order to reach chemical equilibrium and ii) deep convection underestimation as well as seasonal cycle uncertainties within the ERA Interim dataset (Škerlak et al., 2014) lead to doubts concerning the exact onset of ozone STE mass flux maximum around the cordillera.

Table 1 undermines the findings of Figure 5. Only austral fall shows significant changes both during day- and night-times. All other seasons show either decreasing (summer) or slight increasing (winter and spring) trends, which are, however, insignificant. In general, differences between nighttime and daytime trends are very low which indicates that TLL is a very good background station with similar ozone levels under free tropospheric conditions and under planetary boundary layer (PBL) influence. Mean ozone mole fractions at TLL only vary between 32.5 and 31.0 ppb during day and night, while other stations located near greater cities (e.g. Eastern US, Bloomer et al. 2010) report up to 50 ppb peak differences between nighttime and daytime. This finding is most probably attributed not only to the remote location, far away from pollutant sources, but also to the high altitude located above the PBL.

The significant increase of ozone in fall cannot be attributed to changes in STE only, which rather show a slight decrease over the same period of time (see Fig. S9). Factors influencing the trend in austral fall may most probably be an increase of biomass burning in and Southeast Asia (e.g. Shi and Yamaguchi, 2014;Verma et al., 2015) and subsequent eastward transport of ozone precursors, which are highest during the months from January to April. The prevailing westerly conditions (see Fig. 3) exclude any sensitivity of ozone mole fractions at TLL to emissions on the South American continent. Rather, the ozone increase may originate from regional pollution from the La Serena region, which – in fall – may get transported upwards due to the PBL height and occasional support by frontal systems. This latter assumption remains, however, hypothetical (see 4.3). A confirmation would require high resolution numerical simulations to resolve the transport in the mountainous terrain of TLL.

Long term trends similar to TLL can also be found at other stations in both the SH and the NH. We have made use of time series from Cape Point, Mace Head and from western US regions (e.g. Yellowstone NP, Lassen, and others), and most of them show a distinct increase in ozone mixing ratios up to the millennial years though mostly larger than at TTL, before showing signs of levelling off (GAW, 2013;Carslaw, 2005;Derwent et al., 2007;Derwent et al., 2013;Baylon et al., 2015;Cooper et al., 2014). TLL is distinct in that the reversal happens rather late, namely after 2010. However, some western US stations still show signs of growing ozone concentrations, as they are downwind of pollutants from eastern Asia. Those stations, sampling air with origin over the Pacific Ocean, may be partly comparable with the TLL station which is as well sampling air from oceanic origin. Furthermore, the emissions of pollutants upwind of the western US coast are by far much higher than the emissions at similar longitudes from southern hemispheric regions. They are moreover prevalent over the whole year (industrial, coal mining and energy production being the greatest sources), compared to those of the SH which are rather to be classified as seasonal peaks from biomass burning. Yet, as the effect of upwind pollutant release is visible in the datasets of the west coast US stations, it is well possible that long term background ozone trends at TLL are also partly driven by pollutants originating from Southeast Asia.

Next, the ozone data from TLL will be discussed jointly with data from other stations before the influence of large-scale phenomena is discussed in chapter 4.3.

4.2 Annual cycles of O_3 at El Tololo, other ground based sites and from ozone sondes

In the following, the ozone data from TLL and other remote sites will be discussed with respect to the time of the ozone maximum during the year as well as the shape and the amplitude of the annual cycle.

Next to TLL, different monitoring stations in the NH (Jungfraujoch [JFJ], Mauna Loa [MLO], K-Puszta [KPS], Payerne [PAY], and Vindeln [VDL]) and in the SH (Arrival Heights [ARH], Baring Head [BHD], Cape Point [CPT], Cape Grim [CGO], Ushuaia [USH], and La Quiaca [LQO]) were analyzed for comparison. Typical averaged annual cycles of selected available data (reduced to 5~~4~~ typical cycles with KPS, summer maximum, TLL, ~~and~~ LQO and MLO, spring maximum and CPT, winter maximum, for more clarity) are illustrated in Fig. 5~~7~~ a) and b), where the annual cycle of NH stations has been shifted by 182 days for comparability purposes to align the seasons for both NH and SH stations.

In order to characterize TLL as a certain type of station, a clustering of the ten stations into characteristic annual cycle categories has first to be done. All investigated ground-based in-situ ozone measurement either show a maximum in winter, spring or summer, mainly for the three following reasons: i) winter maxima can be mainly seen in clean, marine environments which are primarily driven by ozone depletion due to negative NOx-anomalies and methyl iodide production in summer (Combrink et al., 1995; or Nzotungicimpaye et al., 2014)~~(Combrink et al. (1995) or Nzotungicimpaye et al. (2014))~~. ii) Spring maxima are mainly influenced by STE of ozone-rich air, influencing the regional chemical composition of air through dynamic forcing. iii) Summer maxima are mainly observed at stations influenced by ozone precursor emissions where photochemical production of ozone is the major process driving the annual ozone cycle.

TLL stands as a good example of a station featuring a spring maximum. An in-depth analysis of the drivers for this maximum is given below.

Photochemical ozone production is mainly following the sine-shaped availability of solar radiation, unless there is a strong seasonal variation in the precursors, e.g. due to biomass burning emissions. Dynamic processes such as the north – south movement of the ITCZ, shifts in synoptic weather patterns, and ozone entrainment by STE can result in less regular patterns, as the time of occurrence of the processes is usually concentrated over a shorter time period. The STE-effect at TLL, visible in Fig. S9, smoothly starts in June, reaches a peak in August, and regresses until December, staying at low levels until May. Little to no STE influence is to be expected during the five months between January to May (see also Sect. 4.3). This is the reason why ozone concentrations at TLL follow a slightly asymmetric course over the year. Hence, in order to understand the annual cycles of ozone “in three dimensions” at different latitudes in the SH, additional data is needed.

Therefore, ozone soundings from 12 SH remote locations (San Cristobal, Natal, Java, Ascension Island, Samoa, Fiji, La Réunion, Irene, Rapa Nui, Macquarie Islands, Ushuaia, and Marambio) have been analyzed. In Fig. 6, a compilation of our analysis of both soundings and ground measurements is illustrated on an x-y-diagram~~, where the x-axis is the latitude of the~~

~~sounding/station, and the y-axis represents the "peak-to-peak"-amplitude of the annual cycle. The size of the circle reflects the altitude of the measurement above sea level, and the intensity of the blue color the timing of the annual ozone maximum~~.

Ozone maxima are generally shifting to later times in the year with increasing altitude, i.e. peaks in the annual cycle at 500hPa occur later than the peaks in the annual cycle at 1000 hPa (see Fig. ~~8~~6). This can to a great extent be explained by the location of the soundings, which are all launched in a marine environment. As we have learned before, in most marine surface ozone time series, a winter maximum prevails (around day 180-220). An ascending sounding will first sample air that is influenced by photochemistry in the marine boundary layer. Thus, the higher a station is above sea level, the larger is the share of stratospheric input of ozone. At high altitudes, peak concentrations of ozone are therefore shifted towards later in the year. However, this picture is perturbed by the fact that i) north of 25°S, little to no STE occurs, and ii) the solar cycle is weak north of 10°S. There, interhemispheric mixing explains the late maximum. This process allows some of the NH pollutants to penetrate into the SH across the intertropical convergence zone (ITCZ). The ITCZ is also located in a region where biomass burning prevails all-year long, leading to a very efficient upward transport of pollutants up to the tropopause. Following the position of the ITCZ, the most intense ozone production via the NO_x-HO_x-VOC cycle occurs late in the year. Therefore, we would expect that the maximum shifts from a summer maximum at the equator to a spring maximum at high latitudes.

This hypothesis is further supported by a majority of the soundings (see Fig. ~~8~~6). Especially for soundings made from 25°S southward down to the polar regions, a clear gradient from late maxima to earlier maxima is recognizable (shift from darker to brighter blues). This observation applies not only to soundings, but also to ground-based measurements. A trend to earlier maxima is observed from LQO to ARH, although a smoother grading (more stations) would be beneficial to solidify our hypothesis. When classifying TLL, which is reaching maximum values around mid-October, it can be noticed that the timing is a bit later than one would expect from extrapolating the ozone sonde measurements, as it is a continental station. Maximum concentrations at CPT, CGO, BRH, USH or ARH are reached far earlier, mainly due to i) the marine influence at the stations and ii) the lack of stratospheric influence down to the surface.

The annual cycle at TLL can best be compared to sonde data taken at similar latitude and height. This is fulfilled best by RNO and FJI. A far weaker peak to peak amplitude is found at the surface station TTL (see Fig. ~~8~~6) than in the free atmosphere. Part of this difference can be explained by the origin of air masses, which is dynamically driven. Focusing on the soundings at Rapa Nui (RAP), during the summer and fall months, a strong high-pressure system with center over the island limits the advection of pollutants from the west, hindering photochemical production of ozone. Later in the season, the high pressure system moves slightly eastward, allowing transport of air masses from the Northwest (Oceania) towards the Southern Pacific and, therefore, advecting biomass burning pollutants from Southeast Asia and Oceania via the zonal wind field. In contrast, the sampled air mass at TLL is to a greater part pristine (see above), preventing strong photolytic ozone production in summer.

4.3 Large-scale influences at TLL

There are several large-scale processes which potentially impact either short-term or long-term ozone variations at TLL. These factors include large-scale advection of air masses either via the subtropical jet or via potential vorticity-cutoffs from the polar jet region, stratosphere-troposphere exchange of ozone-rich air from the stratosphere, as well as pattern changes in tropical up- or downwelling. The impact of these different elements vary not only over the course of a day (storm-scale) or of a year (seasonal cycles), but may also oscillate over timescales of two to seven years, following teleconnections and large-scale oscillations from features like the quasi biennial oscillation (QBO) or ENSO.

All these influences are visible in the different ozone data products from TLL. We initially focus on the changes in the mean annual cycle of ozone over time and, based on this, elaborate further on the timing of the maximum and on the shape of the cycle. We conclude this section with a short overview of the observed short-term variations (week-scale) including a possible interpretation for those findings.

First, two mean seasonal cycles for two 5-year periods, one at the beginning of the measurements (1996-2000), and the other one in the recent past (2011-2015), were analyzed for potential differences. In Figure 7, the monthly means, with the upper 95th and the lower 5th percentiles including associated uncertainties are presented. Table 1 summarizes the findings in numbers. The two periods show a very similar annual cycle. However, there are subtle differences: Especially in austral fall (February-March), the 5^{th} percentile, mean, and the 95^{th} percentile increased remarkably from the first to the second period. Among the three curves, the 5^{th} percentile shows the most persistent increase from February up to June in the more recent period. For the other months of the year, changes are minor except for October, where 2011-15 shows slightly lower values of O_3. The annual cycle and some of the differences between the two periods are mainly driven by the annual cycle of ozone STE mass flux (see Fig. 8 and Fig. S9 in the supplementary material). However, the increase of ozone mole fractions from March to May cannot be explained by STE only, as at that time, ozone STE mass flux shows negative anomalies (Fig. S9). Here, three other factors like QBO or ENSO, change in large-scale dynamics and precursor species have to be taken into account. i): As Neu et al. (2014) showed, positive QBO shear and the multivariate ENSO index (MEI) lead to increased stratospheric air circulation, negative upper troposphere ozone anomalies (due to upwelling of relatively ozone-depleted air) and therefore to potentially decreased ozone-STE activity in the sub- and extratropics. Doherty et al. (2006) and Sekiya and Sudo (2012) explained the decrease in total column ozone found in the eastern Pacific region during El Niño conditions with a decrease in NOx-production due to a decrease in lightning activity. The ozone anomalies at TLL and the MEI show significant correlations especially in September-October (cor=-0.78), and the annual cycles of ozone during El Niño years and La Niña years indeed show significantly different values especially in austral fall and spring (Fig. 10). During La Niña events, ozone levels reach higher values – especially from September to November – than during El Niño events. Fig. S10 in the supplementary material illustrates that the 1996-2000 period not only had a weak positive correlation (cor=0.28) of both (QBO shear/MEI) indexes, but also had one single strong El Niño event lasting nearly two years, possibly leading to a decreased ozone-STE burden in 1997/1998. The second, later period showed nearly no in-phase correlation of MEI and

QBO shear index (cor=-0.04) and no significant El Niño event. ii): The subtropical jet has to be considered as contributing factor to the MAM anomaly in the 2011-2015 period. We assume that with the broadening of the Hadley Cell (HC, Choi et al., 2014;Nguyen et al., 2013), the extratropical jet, moving to higher latitudes, increasingly advected more polluted air from Southeast Asia, e.g. in form of Peroxyacetylenitrate (PAN, Jiang et al., 2016) during this period of the year, when biomass burning prevails (e.g. Streets et al., 2003). More work has to be done to confirm this theory, e.g. using satellite measurements, as this would go beyond the scope of this work. iii): An increase of biomass burning in Southeast Asia (e.g. Shi and Yamaguchi, 2014;Verma et al., 2015) and Australia (Cooper et al., 2014) with subsequent eastward transport of ozone precursors, could also explain the positive anomaly in MAM in the 2011-2015 period, as the Northward migration of the ITCZ during this time of the year starts to allow effects of NH emissions to be seen in the SH and prevailing westerly conditions (see Fig. 2) exclude any sensitivity of ozone mole fractions at TLL to emissions on the South American continent. At most, the ozone increase may originate from regional pollution from the La Serena region, which – in fall – may get transported upwards due to the PBL height and occasional support by frontal systems. This latter assumption remains, however, hypothetical. A confirmation would require high-resolution numerical simulations to resolve the transport in the mountainous terrain of TLL. In summary, we conclude that the annual cycle is mostly STE-driven from June to January. From February to April however, the broadening of the HC with subsequent transport of pollutants from Southeast Asia, the contrast to El Niño dominated (1996-2000) versus average years (2011-2015) and the increase in precursor species in Southeast Asia are the best explanations for the positive ozone anomaly in the more recent period. From Table 1, we conclude furthermore that in general, differences between nighttime and daytime trends are very low which indicates that TLL is a very good background station with similar ozone levels under free tropospheric conditions and under planetary boundary layer (PBL) influence. Mean ozone mole fractions at TLL only vary between 32.5 and 31.0 ppb during day and night, while other stations located near greater cities (e.g. Eastern US, Bloomer et al., 2010) report up to 50 ppb peak differences between nighttime and daytime. This finding is most probably attributed not only to the remote location, far away from pollutant sources, but also to the high altitude located above the PBL.

Regarding the 2-month lag between the recent maximum of STE ozone mass flux and the recent maximum of ozone mixing ratio in Figs. 7 vs. S9, we explain this delayed response of ozone to STE by following mechanisms: i) a certain amount of time is needed to equally distribute ozone stemming from STE in the lower troposphere (e.g. titration of NOx & HOx residing in the atmosphere) in order to reach chemical equilibrium and ii) deep convection underestimation as well as seasonal cycle uncertainties within the ERA Interim dataset (Škerlak et al., 2014) lead to doubts concerning the exact onset of ozone STE mass flux maximum around the cordillera.

What concerns the timing of the maximum, Fig. 8 shows a strong correlation (cor=0.89) between the mean annual cycle of STE trajectories (Škerlak, 2014) and of the ozone concentration. The two parameters show a strikingly similar pattern, indicating that STE may be a strong driver for O_3. Note that the "mass flux into the PBL" illustrated in Fig. S9 shows a slightly earlier peak occurrence than the number of "STE trajectories". Another indication for the coupling of O_3 concentration and STE is a coherent shift in the maximum of these quantities over the observation period towards an earlier

occurrence in the year. This is illustrated in Fig. 9. For calculation, a 4-year sliding window of daily data was defined and run over all data between 1996 and 2015. Then, an empirical mode decomposition was done (Huang and Wu, 2008;Wu and Huang, 2009). Out of the Hilbert periodogram, the IMF resembling the most to an annual cycle is selected and the IMF-datapoints are extracted. The latter are averaged to get an average of IMF over the 4-year window. Finally, the day-of-year matching the maximum value of the IMF is extracted. For the ozone time series, a regression of -10 days per decade was calculated. For STT, an even larger trend of -11 or -21 days per decade was obtained for the maximum number of trajectories of stratospheric origin and for the mass flux into the PBL, respectively. Note that the regression is only poorly visible in Fig. 7, where data are aggregated in monthly bins and a comparison of 3 different percentiles of 5-year-monthly averages, instead of absolute maximal values, is shown.

This shift in the seasonal cycle to earlier times in the year has already been presented in other studies for other locations (Parrish et al., 2013; Lin et al., 2014). For instance, spring peaks are observed in the NH to regress with a rate of 3 to 14 days per decade (Parrish et al., 2013). Parrish et al. (2013) also suggest that the relative contribution from the stratosphere may at least partly explain the shift in the annual cycle at high-altitude stations in the NH like Jungfraujoch, being located at 3580 meters asl. Yet, a conclusive explanation for this shift of the seasonal cycle remains missing. Schnell et al. (2016) recently suggested that future climate change will shift the maximum of the ozone seasonal cycle to earlier in the year, but they did not provide any clear explanation for this phenomenon.

Considering the short-term variations, it is known from previous studies that a (anti)correlation between ozone and relative humidity exists at TLL, but only in very specific cases. Gallardo et al. (2000), analyzing the first years of data collected at Tololo, found such an anticorrelation between ozone and water vapor in summer in connection with upslope transport of boundary layer air associated with a thermally driven circulation. Rondanelli et al. (2002) investigated the effect of troughs associated with a frontal zone passing over TLL, and could classify their observations in two categories: wet and dry events. During wet events, relatively humid air from the PBL is advected to TLL, and shortly after regression of relative humidity, ozone is rising rapidly. During dry events, ozone is rising, but relative humidity stays at normal, dry levels or drops even further. Carbon monoxide, a good PBL pollutant and hence an optimal tracer, has been measured in TLL since April 2013. Therefore, the dependence of CO and ozone was investigated. This analysis revealed a significant correlation (not shown) in rare, specific episodes, during which less pristine air from the PBL – originating from the La Serena, Valparaiso and Santiago regions – is reaching TLL. Those events were not always associated with low potential vorticity values (PV streamer, reconstructed from ERA Interim data, not shown) or frontal zones, but some of them were. This confirms the finding of Rutllant et al. (2013), who, during the VOCALS-REx-campaign, found a persistent, regular South-Westerly advection via thermals, being able to transport air masses in the afternoon from the marine region into the Andes which would allow inbound transport of slightly more polluted air masses to TLL. An in-depth analysis of CO-O_3-correlations over several years may be promising to provide more robust conclusions. However, the CO time series is still limited in time and an extended study would go beyond the scope of the paper.

The uniqueness of the seasonal cycle at TLL is linked to large scale dynamics and subsequent cycles in STE. While it is difficult to discern the "signature" of stratospheric ozone from tropospheric ozone, Figs. 9 and 10 provide some indication that STE and associated ozone entrainment is a key driver for the observed ozone variability and trend at TLL. Fig. 9 shows the annual cycle of ozone concentration and the transport of air masses from the stratosphere. The latter are numbers averaged over 18 years and are extracted from the Škerlak et al. (2014) climatology. The two parameters show a strikingly similar patter, indicating that, in fact, STE may be a strong driver for O_3. Another indication for the coupling of O_3 concentration and STE is a coherent shift in the maximum of these quantities over the observation period towards an earlier occurrence in the year. This is illustrated in Fig. 10. For calculation, a 4-year sliding window of daily data was defined and run over all data between 1996 and 2015. Average values for the years 1996-1999 are shown as the data point in end of December 1997, 1997-2000 in end of December 1998, and so forth until years 2012-2015 which are shown as data point in end of December 2013. Then, an empirical mode decomposition was done (Huang and Wu, 2008;Wu and Huang, 2009). Out of the Hilbert periodogram, the IMF resembling the most to an annual cycle is selected and the IMF datapoints are extracted. The latter are averaged to get an average of IMF over the 4 year window. Finally, the day of year matching the maximum value of the IMF is extracted. For the ozone time series, a regression of -10 days per decade was calculated. For STT, an even larger trend of -11 or -21 days per decade was obtained for the maximum number of trajectories of stratospheric origin and for the mass flux into the PBL, respectively.Note that the regression is only poorly visible in Fig. 5, in which data are aggregated in monthly bins and a comparison of 3 different percentiles of 5 year monthly averages, instead of absolute maximal values, is shown.

Again, this evaluation of yearly maxima shows a strong resemblance between ozone volume mixing ratio and stratospheric influences for both STE trajectories and mass fluxes into the PBL. Overall, we conclude that there are strong indications that the annual cycle at TLL is to a major part driven by STE.

The shift in the seasonal cycle has already been presented in other studies for other locations (Parrish et al., 2013;Lin et al., 2014). For instance, spring peaks are observed in the NH to regress with a rate of 3 to 14 days per decade (Parrish et al., 2013). Parrish et al. (2013) also suggest that the relative contribution from the stratosphere may at least partly explain the shift in the annual cycle at high altitude stations in the NH like Jungfraujoch, being located at 3580 meters asl. Yet, a conclusive explanation for this shift of the seasonal cycle remains missing. Schnell et al. (2016) recently suggested that future climate change will shift the maximum of the ozone seasonal cycle to earlier in the year, but they did not provide any clear explanation for this phenomenon.

As TLL does represent a special case, it is of interest to also look at other modes of O3 variability. We will first summarize short term variation patterns. Then, the dependence of O3 on large scale, long term oscillating patterns like the El Niño southern oscillation will be discussed.

Concerning short term variations, it is known from previous studies that a (anti)correlation between ozone and relative humidity exists at TLL, but only in very specific cases. Gallardo et al. (2000), analyzing the first years of data collected at Tololo, found such an anticorrelation between ozone and water vapor in summer in connection with upslope transport of

boundary layer air associated with a thermally driven circulation. Rondanelli et al. (2002) investigated the effect of troughs associated with a frontal zone passing over TLL, and could classify their observations in two categories: wet and dry events. During wet events, relatively humid air from the PBL is advected to TLL, and shortly after regression of relative humidity, ozone is rising rapidly. During dry events, ozone is rising, but relative humidity stays at normal, dry levels or drops even further. This study partly confirmed our finding of 4.1, where we explain the seasonal cycle with partial PBL influence. Carbon monoxide, a good PBL pollutant and hence an optimal tracer, has been measured in TLL since April 2013. Therefore, the dependence of CO and ozone was investigated. This analysis revealed a significant correlation (not shown) in rare, specific episodes, during which less pristine air from the PBL – originating from the La Serena, Valparaiso and Santiago regions – is reaching TLL. Those events were not always associated with low potential vorticity values (PV streamer, reconstructed from ERA Interim data, not shown) or frontal zones, but some of them were. This confirms the finding of Rutllant et al. (2013), who, during the VOCALS REx campaign, found a persistent, regular South Westerly advection via thermals, being able to transport air masses in the afternoon from the marine region into the Andes which would allow inbound transport of slightly more polluted air masses to TLL. An in depth analysis of CO-O_3 correlations over several years would go beyond the scope of the paper, however would provide more robust conclusions.

On longer time scales, also ENSO is known to dramatically influence climate variables in entire South America with a frequency of 3-5 years. This is the amount of time needed by the global climate system to switch from an El Niño phase to a La Niña phase. Although the ozone anomalies at TLL and the ENSO index do not show any significant correlation, annual cycles of ozone during El Niño years and La Niña years show significantly different values especially in austral fall and spring (Fig. 11). During La Niña events, ozone levels reach higher values especially from September to November than during El Niño events. During La Niña years the Pacific high is stronger, which leads to more subsidence allowing the downward mixing of ozone rich air from the upper troposphere possibly connected with STE processes. On the contrary, El Niño years result in a weaker Pacific high and in diminished subsidence. Moreover, based on Fig. 4 in section 2.1, the strengthening of the low-level southerly flow during La Niña events may allow air parcels from the greater Santiago area to reach TLL more easily than during El Niño years. Also, cooler conditions during La Niña years may allow transport of PAN over larger distances. PAN can act as a reservoir for organic nitrates and releases nitrogen oxides after thermal decomposition which can lead to an efficient production of ozone in pristine environments such as TLL (see e.g. Fischer et al. (2014)). Lastly, large scale anomalies of meteorological conditions over the Pacific could be the major driver of the differences during El Niño and La Niña conditions. As shown in the modelling studies of Doherty et al. (2006) and Sekiya and Sudo (2012), decrease in total column ozone is found in the eastern Pacific region during El Niño conditions. They attribute that to a decrease in NOx production due to less lightning. It is highly probable that this has an effect on the ozone cycles of TLL illustrated in Fig. 11 also. Currently, the lower NOx values in the TLL region during El Niño events cannot be confirmed due to missing measurements.

5 Conclusions

The 20 year-long surface ozone time series of El Tololo, Chile (TLL) has been presented and analyzed. It was characterized and put into a global context with the help of Stratosphere-Troposphere-Exchange (STE) climatology, trajectory analysis, surface ozone data from other stations, as well as ozone soundings. The analysis shows that El Tololo represents a remote measuring site in a pristine setting, which rarely gets influenced by local pollution, and thus represents an excellent remote GAW station. An indication of this is the relatively small amplitude of the diurnal cycle, even in summer.

The following bullet points summarize the most important conclusions:

- Only a few data gaps exist in the 20-year-long ozone dataset
- A positive trend of +0.66 ppb/decade is found up to recent years, which gets weaker from 2010 on and possibly reverses in 2011
- Over the entire period, the strongest increase in ozone concentrations is observed in austral fall, the strongest decrease in austral summer. ~~The latter~~Th~~-~~is most probably is related to different origins of the air masses ~~and greater influence of the Santiago and La Serena region in fall (March-May) than in summer (December-February)~~ and to an increase in precursor species over Southeast Asia.
- In general, the average annual cycle at TLL is dominated by peak concentrations in late spring, followed by a sharp decrease in late winter to early fall, correlating with the shape of average annual STE. TLL can, therefore, be mainly classified as a STE-influenced station, in contrast to stations that are in the marine-boundary-layer or significantly influenced by anthropogenic-pollution.
- Characterizing the TLL data set with the help of ozone soundings makes it possible to see that the free-tropospheric influence is very strong compared to other stations
- The maximum ozone concentrations were reached around week 41 (early October) in 1996 and have been retrograding since; recently, maximum concentrations are reached around week 38 (-10 days per decade). This is attributed to a retrogradation in the same magnitude of the maximum in the ST mass flux into the PBL (-21 days per decade) and of the number of STE trajectories around El Tololo (-11 days per decade).
- The ozone concentrations at El Tololo are ENSO-sensitive. Over the entire year, ozone concentrations are higher during La Niña conditions than during El Niño conditions, especially in late austral spring. This is related to ~~the~~ large-scale atmospheric circulation anomalies over the Pacific, changing the strength of the tropical upwelling and coming along with less NOx-production by lightning and changing circulation patterns.

While many aspects of the O_3 time series are well explained, two observations remain unclear and may be elucidated ~~in~~ with the help of regional and a global modelling studies. Firstly, the origin of the retrogradation of the timing of ozone STE maximum is yet unclear. Our hypothesis is that large-scale gravity wave momentum transport has changed over years due to changing tropopause height. Secondly, different ozone trends for different seasons (austral fall versus austral summer) are observed. While part of it can be explained with an increase in precursor species during the biomass burning season over

Southeast Asia, ~~W~~we postulate that a second explanation ~~might be~~ that polluted air masses from the greater Santiago area are transported northwards up to La Serena, where the local wind systems (Elqui-Valley-wind) transports the plume up to El Tololo. This process has been confirmed by a short preliminary study with a regional model. At least one year of high-resolution regional model results is required to be able to confirm or reject this hypothesis.

Acknowledgements

We acknowledge the support of the Federal Office of Meteorology and Climatology MeteoSwiss through the project Capacity Building and Twinning for Climate Observing Systems (CATCOS) Phase 2, Contract no. 81025332 between the Swiss Agency for Development and Cooperation (SDC) and MeteoSwiss. Moreover, we would like to express our gratitude towards Michael Sprenger and Bojan Skerlak, who both advised us how to use their ozone STE climatology. As well, we thank Dr. Stephan Henne for his support concerning the FLEXTRA datasets and Dr. Dominik Brunner for his valuable comments. Laura Gallardo is grateful for the support of FONDAP 15110009.

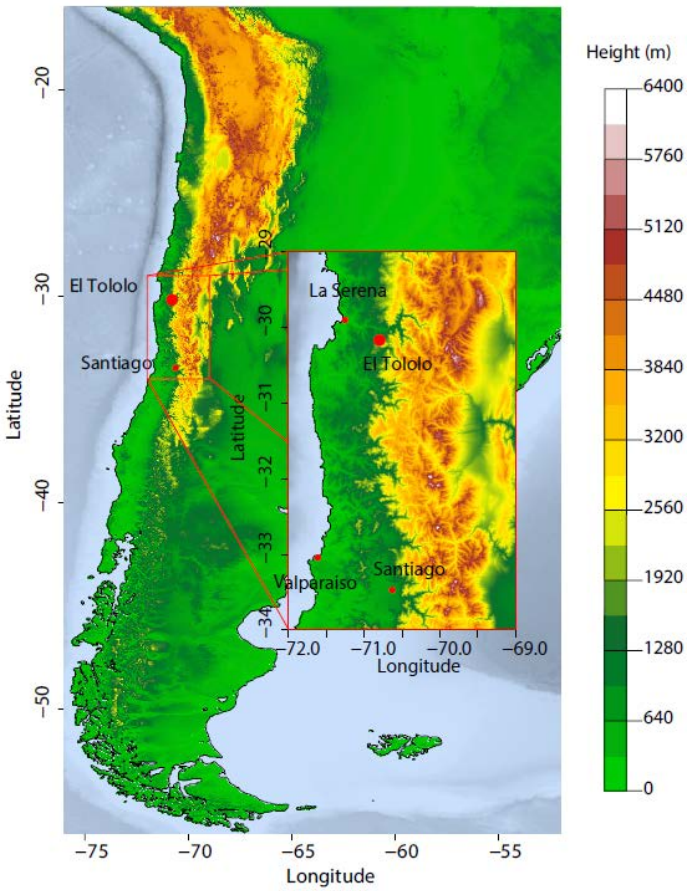

Figure 1: Position of El Tololo, La Serena, Valparaiso and Santiago de Chile including topographic information. Terrain data source: NOAA ETOPO1, plotted using marmap (Pante and Simon-Bouhet, 2013).

5

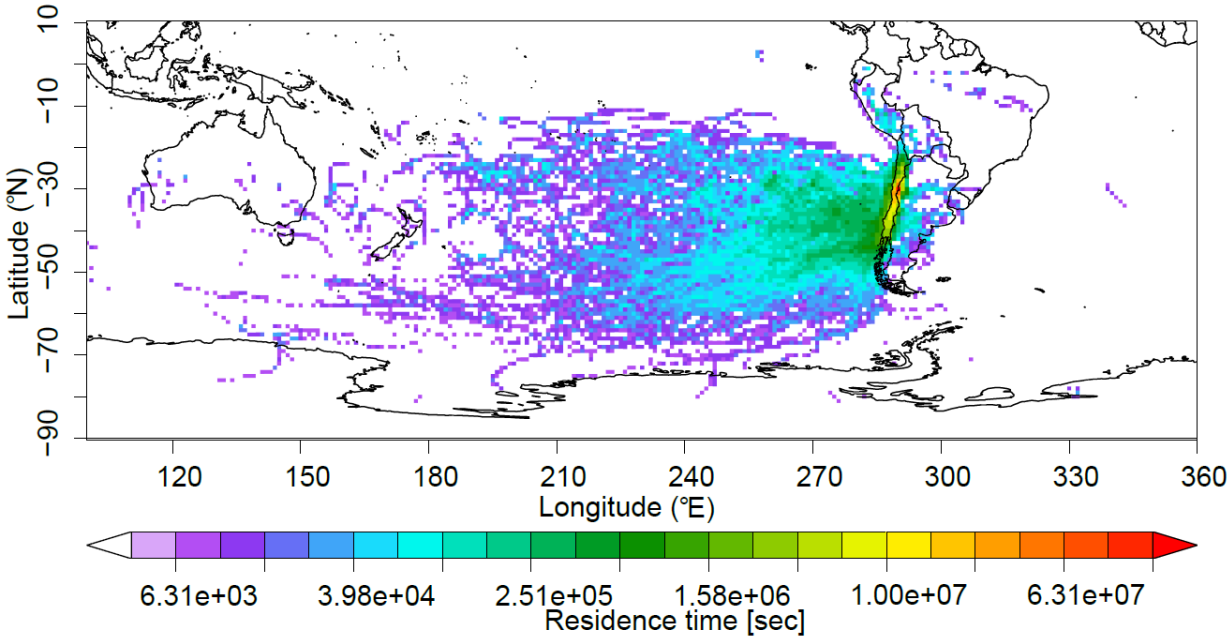

Figure 2: FLEXTRA trajectory footprint from April 2013- December 2015, origin: TLL, 370m above model topography. Color indicates the total residence time of air parcels, summed up over the time period. TLL is marked with a black dot.

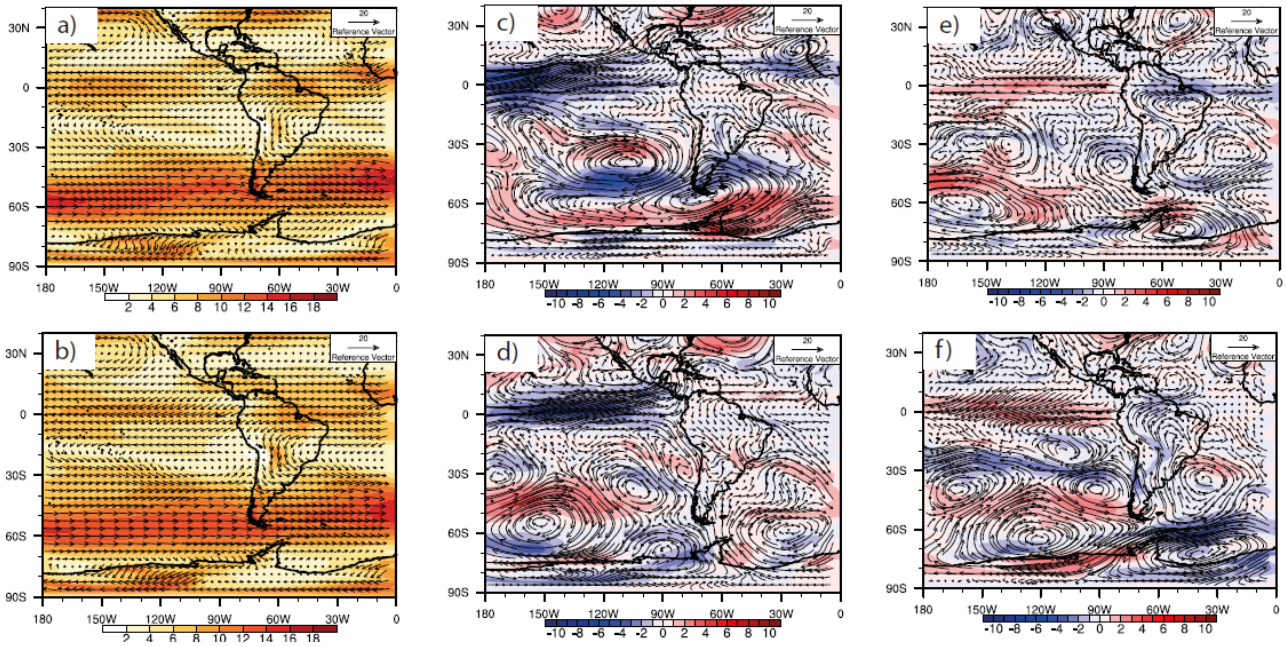

Figure 3: ERA Interim wind climatology at 700 hPa (a, MAM and ~~&~~ b, SON) and wind change in vector and strength during an exemplary El Niño event (1997-1998) (~~c &~~ dc, MAM and d, SON) and a La Niña event (1988-1989) (e, MAM and f, SON~~e & f~~).

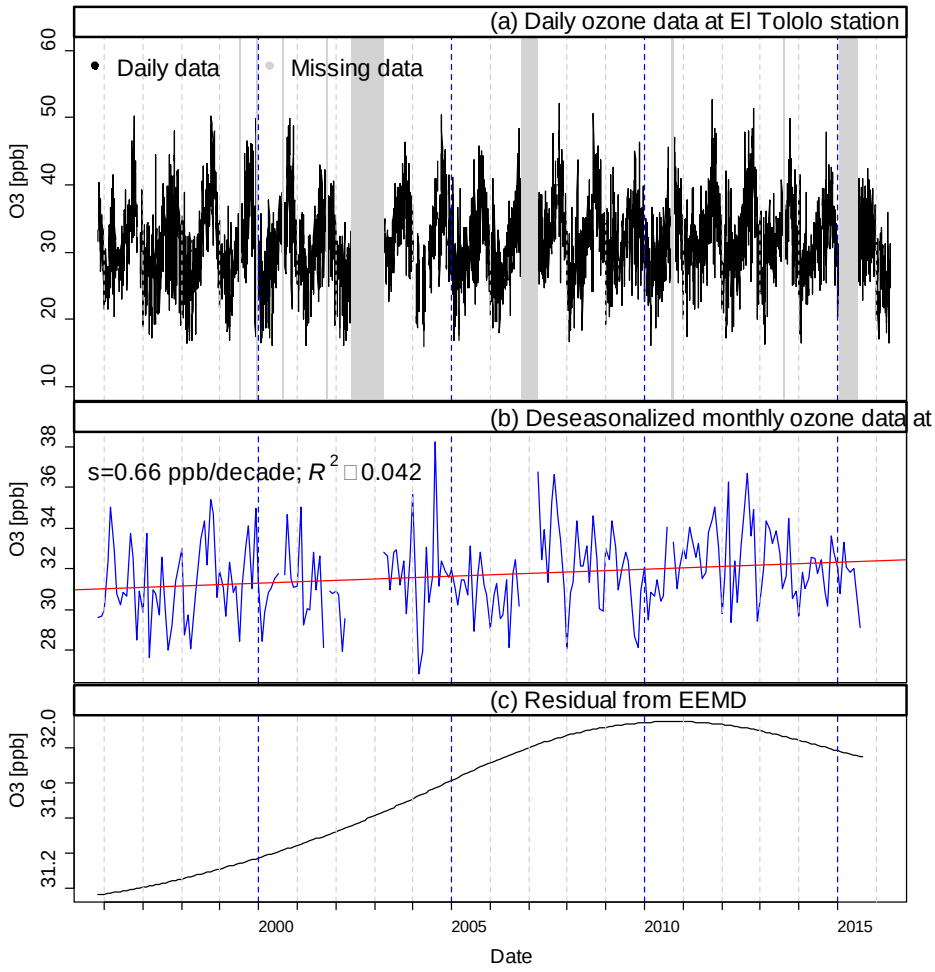

Figure 4: Time series of (a) hourly ozone mole fractions at TLL (black) and data gaps (grey); (b) deseasonalized monthly means of ozone mole fractions at TLL (blue) with linear fit (red). Slope of the linear fit is 0.66 ppb/decade; (c) residual trend of the EEMD decomposition.

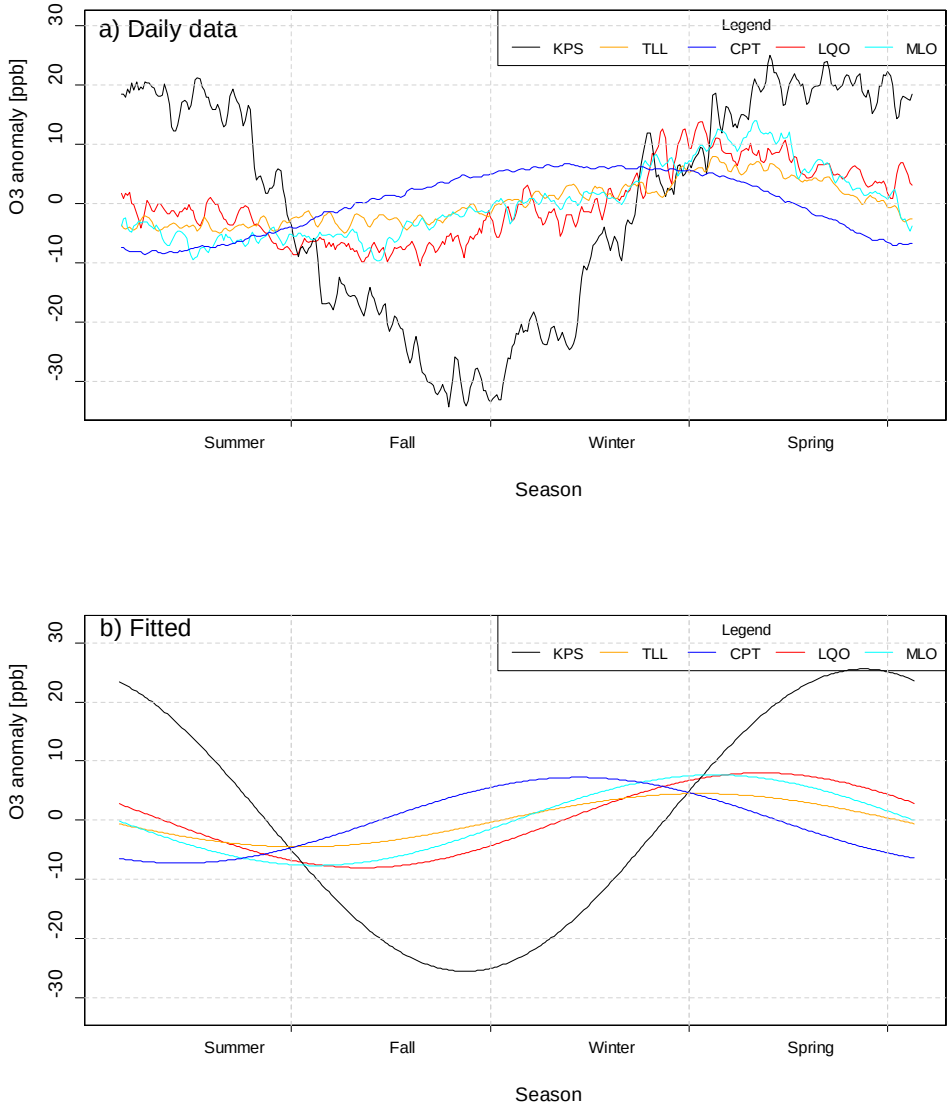

Figure 5: a) Mean annual cycle of ozone anomalies at different background stations showing a spring maximum (El Tololo [TLL], La Quiaca [LQO], Mauna Loa [MLO]), a summer maximum (K-Puszta [KPS]) or a summer minimum (Cape Point [CPT]). Anomalies are deviations from the annual mean. The x-axis shows the day of year. Northern hemispheric data are shifted by 182 days. b) Sine fit to the annual cycles shown in a).

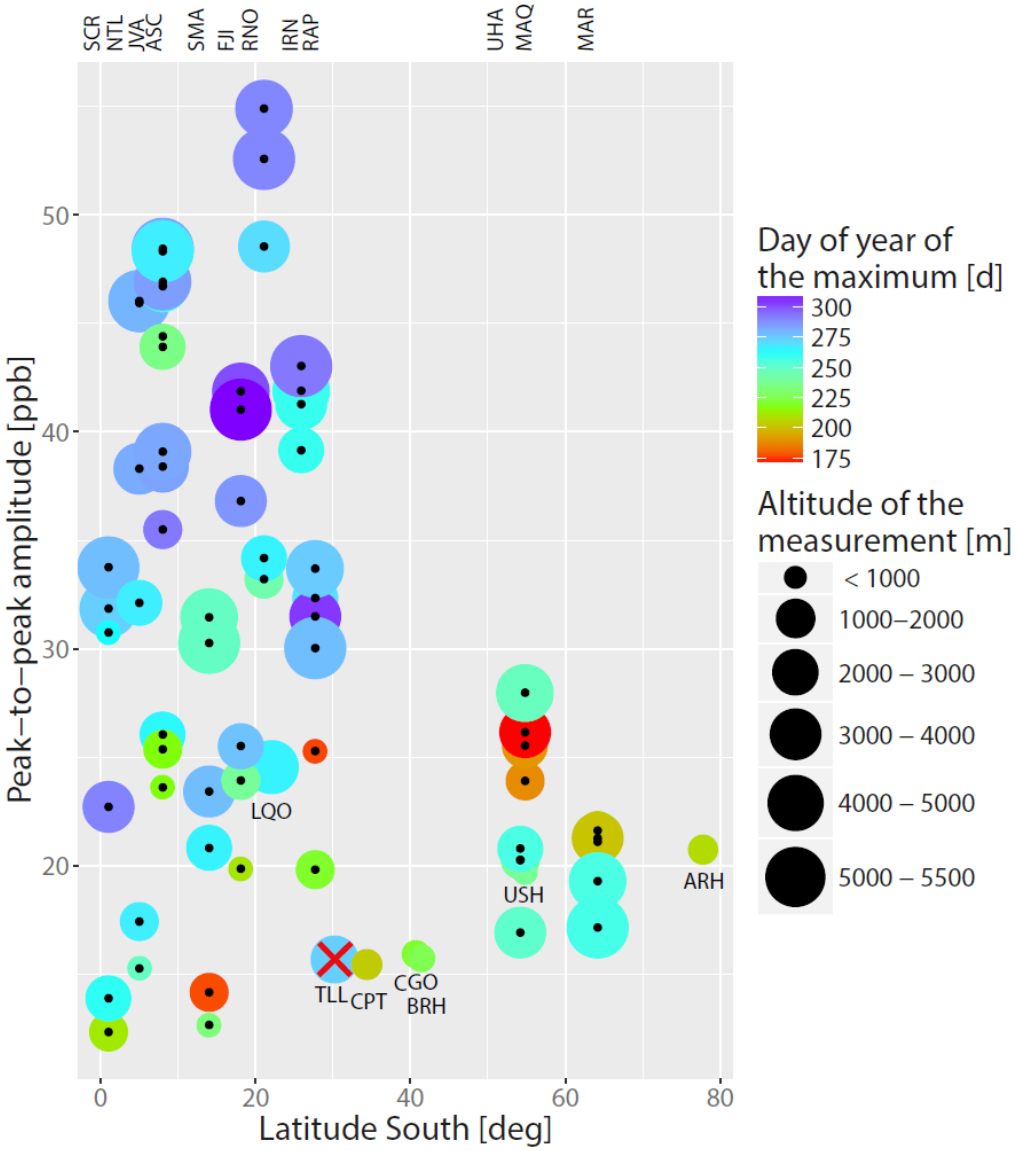

Figure 6: Composite plot showing the different southern hemispheric ozone measurements (SHADOZ and WOUDC network and ground-based in-situ data): the x-axis shows the southern latitude, the y-axis represents the delta between the maximum and the minimum of the annual cycle ("Peak-to-peak amplitude"). The size of the points represents the height of the station (ground-based) or of the ozone sonde measurement (SHADOZ & WOUDC). The colors depict the day of year when the maximum of the annual cycle is reached. Points with a black spot illustrate sonde measurements. TLL can be seen at 30°S and an amplitude of 15ppb.

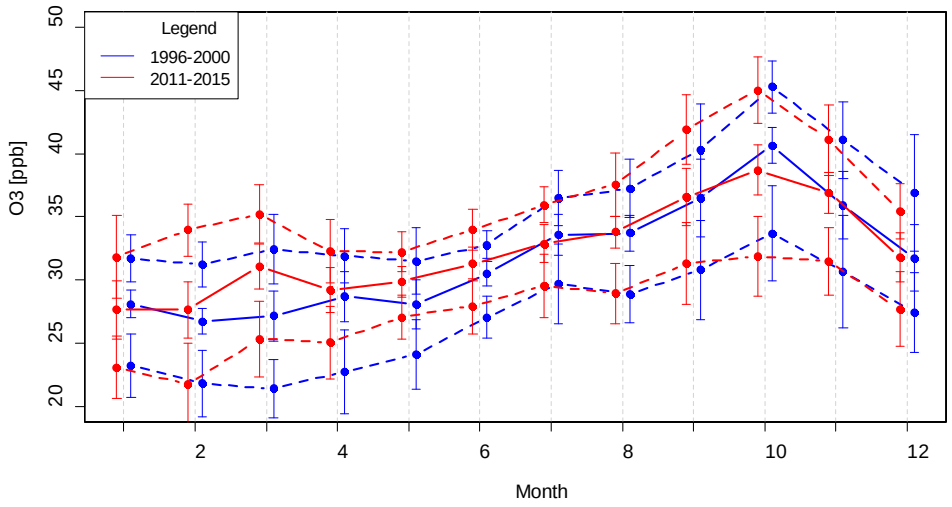

Figure 7: Mean annual cycles of ozone mole fraction (1996-2000 and 2011-2015) showing mean, upper 95th percentile and lower 5th percentile. For better readability, the monthly means for both periods have been shifted by ±7 days.

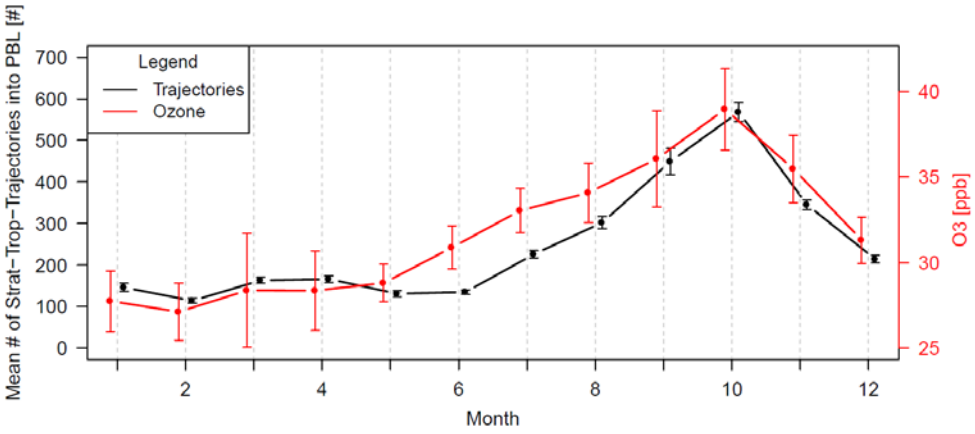

Figure 8: Mean annual cycle over 1~~8~~9 years (1996 - 2015) of ozone at TLL and of trajectories indicating STE above TLL.

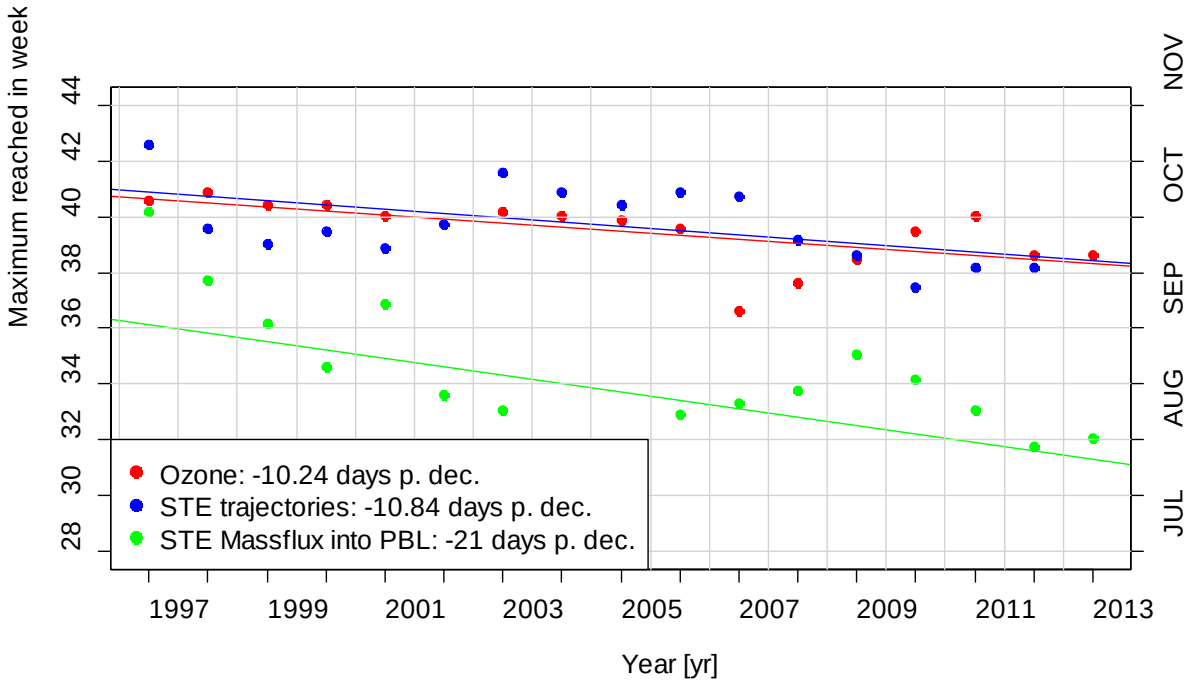

Figure 9: Time of the year, for which the maximum of ozone (red), STE trajectories (blue), and STE mass flux into the PBL (green) is reached. A 4-year sliding window of daily data was applied. Average values for the years 1996-1999 are shown as the data point in end of December 1997, 1997-2000 in end of December 1998, and so forth until years 2012-2015 which are shown as data point in end of December 2013.

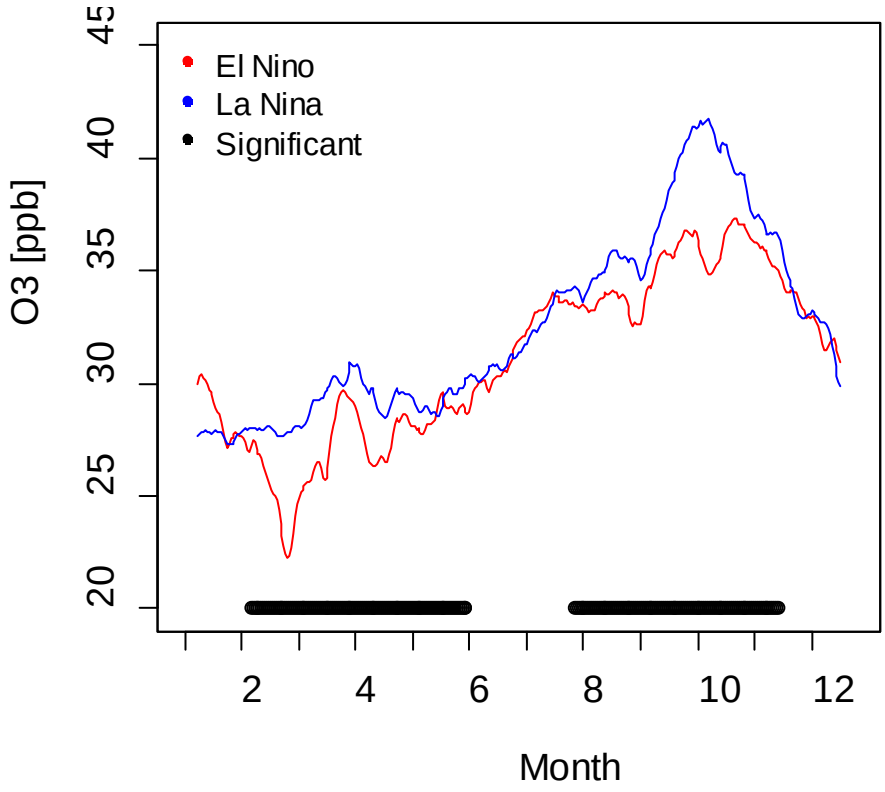

Figure 10: Computed annual cycle of O_3 mole fractions at TLL in daily resolution during El Niño days (NINO3.4-Index >0.5, total 1914 days between December 1995 and December 2015) and La Niña days (NINO3.4-Index < -0.5, total 2330 days between December 1995 and December 2015). Black point show significant differences between the two curves. NINO3.4 data is derived from daily index reconstructions from SST OI v2 1/4 degree data by NOAA.

Table 1: Seasonal linear trends of ozone [ppb / decade] at TLL for a) all-day data (00 to 24 UTC), b) nighttime data from 10 PM to 4 AM, and c) daytime data from 11 AM to 5 PM. Significant trends are labelled with ** (95%) or * (90%) ~~(95%).~~, standard error is shown as ±

Time of day / Season	DJF	p-value	MAM	p-value	JJA	p-value	SON	p-value
all	-0.1~~2~~±0.05	0.619	1.6**±0.06	0.0353	0.2±0.04	0.855	0.1±0.07	0.881
nighttime	-0.03~~5~~±0.06	0.843	1.~~5~~8**±0.07	0.0271	0.3±0.04	0.745	0.1~~5~~±0.07	0.821
daytime	-0.~~43~~±0.05	0.231	1.2~~9~~**±0.06	0.0909	0.1~~5~~±0.01	0.866	0.1~~7~~±0.06	0.802

References

Ayers, G. P., Penkett, S. A., Gillet, R. W., Bandy, B., Galbally, I. E., Meyer, C. P., Elsworth, C. M., Bentley, S. T., and Forgan, B. W.: Evidence for photochemical control of ozone concentrations in unpolluted marine air, Letters to Nature, 360, 446-449, 1992.

Barlasina, M. E., Carbajal Benitez, G., Copes, G., Demasi, M., and Cupeiro, M.: Estudio del ozono troposférico en tres observatorios de la red de medición del servicio meteorológico nacional – argentina, http://www.congremet.prmarg.org/upload/barlasinamaelena.pdf, 2013.

Baylon, P., Jaffe, D. a., Wigder, N. L., Gao, H., and Hee, J.: Ozone enhancement in western US wildfire plumes at the Mt. Bachelor Observatory: The role of NOx, Atmospheric Environment, 109, 297-304, 10.1016/j.atmosenv.2014.09.013, 2015.

Brook, R. D.: Inhalation of Fine Particulate Air Pollution and Ozone Causes Acute Arterial Vasoconstriction in Healthy Adults, 105, 1534-1536, 10.1161/01.CIR.0000013838.94747.64, 2002.

Carslaw, D. C.: On the changing seasonal cycles and trends of ozone at Mace Head, Ireland, Atmospheric Chemistry and Physics Discussions, 5, 5987-6011, 10.5194/acpd-5-5987-2005, 2005.

Choi, J., Son, S.-W., Lu, J., and Min, S.-K.: Further observational evidence of Hadley cell widening in the Southern Hemisphere, Geophysical Research Letters, 41, 2590-2597, 10.1002/2014GL059426, 2014.

Collins, W. J., Derwent, R. G., Garnier, B., Johnson, C. E., Sanderson, M. G., and Stevenson, D. S.: Effect of stratosphere-troposphere exchange on the future tropospheric ozone trend, Journal of Geophysical Research: Atmospheres, 108, n/a-n/a, 10.1029/2002JD002617, 2003.

Combrink, J., Diab, R. D., Sokolic, F., and Brunke, E. G.: Relationship between surface, free tropospheric and total column ozone in two contrasting areas in South Africa, Atmospheric Environment, 29, 685-691, http://dx.doi.org/10.1016/1352-2310(94)00313-A, 1995.

Cooper, O. R., Gao, R. S., Tarasick, D., Leblanc, T., and Sweeney, C.: Long-term ozone trends at rural ozone monitoring sites across the United States, 1990-2010, Journal of Geophysical Research: Atmospheres, 117, 1990-2010, 10.1029/2012JD018261, 2012.

Cooper, O. R., Parrish, D. D., Ziemke, J., Balashov, N. V., Cupeiro, M., Galbally, I. E., Gilge, S., Horowitz, L., Jensen, N. R., Lamarque, J. F., Naik, V., Oltmans, S. J., Schwab, J., Shindell, D. T., Thompson, a. M., Thouret, V., Wang, Y., and Zbinden, R. M.: Global distribution and trends of tropospheric ozone: An observation-based review, Elementa: Science of the Anthropocene, 2, 000029-000029, 10.12952/journal.elementa.000029, 2014.

Crutzen, P.: A discussion of the chemistry of some minor constituents in the stratosphere and troposphere, pure and applied geophysics, 106, 1385-1399, 10.1007/bf00881092, 1973.

Crutzen, P. J.: Ozone production rates in an oxygen-hydrogen-nitrogen oxide atmosphere, 76, 7311-7311, 10.1029/JC076i030p07311, 1971.

Crutzen, P. J., and Zimmermann, P. H.: The changing photochemistry of the troposphere, Tellus B, 43, 136-151, 10.1034/j.1600-0889.1991.t01-1-00012.x, 1991.

Derwent, R. G., Jenkin, M. E., Saunders, S. M., and Pilling, M. J.: Photochemical ozone creation potentials for organic compounds in northwest Europe calculated with a master chemical mechanism, Atmospheric Environment, 32, 2429-2441, http://dx.doi.org/10.1016/S1352-2310(98)00053-3, 1998.

Derwent, R. G., Simmonds, P. G., Manning, a. J., and Spain, T. G.: Trends over a 20-year period from 1987 to 2007 in surface ozone at the atmospheric research station, Mace Head, Ireland, Atmospheric Environment, 41, 9091-9098, 10.1016/j.atmosenv.2007.08.008, 2007.

Derwent, R. G., Manning, A. J., Simmonds, P. G., Spain, T. G., and O'Doherty, S.: Analysis and interpretation of 25 years of ozone observations at the Mace Head Atmospheric Research Station on the Atlantic Ocean coast of Ireland from 1987 to 2012, Atmospheric Environment, 80, 361-368, http://dx.doi.org/10.1016/j.atmosenv.2013.08.003, 2013.

Doherty, R. M., Stevenson, D. S., Johnson, C. E., Collins, W. J., and Sanderson, M. G.: Tropospheric ozone and El Niño–Southern Oscillation: Influence of atmospheric dynamics, biomass burning emissions, and future climate change, Journal of Geophysical Research: Atmospheres, 111, n/a-n/a, 10.1029/2005JD006849, 2006.

Elshorbany, Y. F., Kleffmann, J., Kurtenbach, R., Rubio, M., Lissi, E., Villena, G., Gramsch, E., Rickard, A. R., Pilling, M. J., and Wiesen, P.: Summertime photochemical ozone formation in Santiago, Chile, Atmospheric Environment, 43, 6398-6407, http://dx.doi.org/10.1016/j.atmosenv.2009.08.047, 2009.

Fischer, E. V., Jacob, D. J., Yantosca, R. M., Sulprizio, M. P., Millet, D. B., Mao, J., Paulot, F., Singh, H. B., Roiger, A., Ries, L., Talbot, R. W., Dzepina, K., and Pandey Deolal, S.: Atmospheric peroxyacetyl nitrate (PAN): a global budget and source attribution, Atmos. Chem. Phys., 14, 2679-2698, 10.5194/acp-14-2679-2014, 2014.

Fiscus, E. L., Booker, F. L., and Burkey, K. O.: Crop responses to ozone: Uptake, modes of action, carbon assimilation and partitioning, 28, 997-1011, 10.1111/j.1365-3040.2005.01349.x, 2005.

Fuenzalida, H. A., Sánchez, R., and Garreaud, R. D.: A climatology of cutoff lows in the Southern Hemisphere, Journal of Geophysical Research: Atmospheres, 110, n/a-n/a, 10.1029/2005JD005934, 2005.

Galbally, I.: Some Measurements of Ozone Variation and Destruction in the Atmospheric Surface Layer, Nature, 218, 456-457, 10.1038/218456a0, 1968.

Gallardo, L., Carrasco, J., and Olivares, G.: An analysis of ozone measurements at Cerro Tololo (30 degrees S, 70 degrees W, 2200 m.a.s.l.) in Chile, Tellus Series B-Chemical and Physical Meteorology, 52, 50-59, 10.1034/j.1600-0889.2000.00959.x, 2000.

Garreaud, R. D., and Muñoz, R. C.: The Low-Level Jet off the West Coast of Subtropical South America: Structure and Variability, Monthly Weather Review, 133, 2246-2261, 10.1175/mwr2972.1, 2005.

GAW: GAW Report No . 209 Guidelines for Continuous Measurements of Ozone in the Troposphere, 2013.

Geiger, R.: Überarbeitete Neuausgabe von Geiger, R: Köppen- Geiger/Klima der Erde.(Wandkarte 1:16 Mill.), Klett-Perthes, Gotha., 1961.

Hegglin, M. I., and Shepherd, T. G.: Large climate-induced changes in ultraviolet index and stratosphere-to-troposphere ozone flux, Nature Geosci, 2, 687-691, http://www.nature.com/ngeo/journal/v2/n10/suppinfo/ngeo604_S1.html, 2009.

Holton, J. R., Haynes, P. H., McIntyre, M. E., Douglass, A. R., Rood, R. B., and Pfister, L.: Stratosphere-troposphere exchange, Reviews of Geophysics, 33, 403-403, 10.1029/95RG02097, 1995.

Huang, N. E., and Wu, Z.: A review on Hilbert-Huang transform: Method and its applications to geophysical studies, Reviews of Geophysics, 46, n/a-n/a, 10.1029/2007RG000228, 2008.

Janssens-Maenhout, G., Crippa, M., Guizzardi, D., Dentener, F., Muntean, M., Pouliot, G., Keating, T., Zhang, Q., Kurokawa, J., Wankmüller, R., Denier van der Gon, H., Kuenen, J. J. P., Klimont, Z., Frost, G., Darras, S., Koffi, B., and Li, M.: HTAP_v2.2: a mosaic of regional and global emission grid maps for 2008 and 2010 to study hemispheric transport of air pollution, Atmos. Chem. Phys., 15, 11411-11432, 10.5194/acp-15-11411-2015, 2015.

Jiang, Z., Worden, J. R., Payne, V. H., Zhu, L., Fischer, E., Walker, T., and Jones, D. B. A.: Ozone export from East Asia: The role of PAN, Journal of Geophysical Research: Atmospheres, 121, 6555-6563, 10.1002/2016JD024952, 2016.

Kalthoff, N., Bischoff-Gauß, I., Fiebig-Wittmaack, M., Fiedler, F., Thürauf, J., Novoa, E., Pizarro, C., Castillo, R., Gallardo, L., Rondanelli, R., and Kohler, M.: Mesoscale Wind Regimes in Chile at 30°S, Journal of Applied Meteorology, 41, 953-970, 10.1175/1520-0450(2002)041<0953:mwrica>2.0.co;2, 2002.

Kendall, M., and Stuart, A.: The Advanced Theory of Statistics, Griffin
1983.

Kottek, M., Grieser, J., Beck, C., Rudolf, B., and Rubel, F.: World map of the Köppen-Geiger climate classification updated, Meteorologische Zeitschrift, 15, 259-263, 10.1127/0941-2948/2006/0130, 2006.

Lefohn, A. S., and Cooper, O. R.: Introduction to the special issue on observations and source attribution of ozone in rural regions of the western United States, Atmospheric Environment, 109, 279-281, 10.1016/j.atmosenv.2015.03.030, 2015.

Lin, M., Horowitz, L. W., Oltmans, S. J., Fiore, A. M., and Fan, S.: Tropospheric ozone trends at Mauna Loa Observatory tied to decadal climate variability, Nature Geosci, 7, 136-143, 10.1038/ngeo2066
http://www.nature.com/ngeo/journal/v7/n2/abs/ngeo2066.html#supplementary-information, 2014.

Lin, M., Fiore, A. M., Horowitz, L. W., Langford, A. O., Oltmans, S. J., Tarasick, D., and Rieder, H. E.: Climate variability modulates western US ozone air quality in spring via deep stratospheric intrusions, Nature Communications, 6, 7105, 10.1038/ncomms8105
http://www.nature.com/articles/ncomms8105#supplementary-information, 2015.

Monks, P.: A review of the observations and origins of the spring ozone maximum, 34, 10.1016/S1352-2310(00)00129-1, 2000.

Muñoz, R. C., and Garreaud, R. D.: Dynamics of the Low-Level Jet off the West Coast of Subtropical South America, Monthly Weather Review, 133, 3661-3677, 10.1175/mwr3074.1, 2005.

Myhre, G., Shindell, D., Bréon, F. M., Collins, W., Fuglestvedt, J., Huang, J., Koch, D., Lamarque, J. F., Lee, D., Mendoza, B., Nakajima, T., Robock, A., Stephens, G., Takemura, T., and Zhan, H.: 2013: Anthropogenic and Natural Radiative Forcing, Climate Change 2013: The Physical Science Basis. Contribution of Working Group I to the Fifth Assessment Report of the Intergovernmental Panel on Climate Change, 659-740, 10.1017/ CBO9781107415324.018, 2013.

Neu, J. L., Flury, T., Manney, G. L., Santee, M. L., Livesey, N. J., and Worden, J.: Tropospheric ozone variations governed by changes in stratospheric circulation, Nature Geosci, 7, 340-344, 10.1038/ngeo2138, 2014.

Nguyen, H., Evans, A., Lucas, C., Smith, I., and Timbal, B.: The Hadley Circulation in Reanalyses: Climatology, Variability, and Change, Journal of Climate, 26, 3357-3376, 10.1175/jcli-d-12-00224.1, 2013.

Nzotungicimpaye, C.-M., Abiodun, B. J., and Steyn, D. G.: Tropospheric ozone and its regional transport over Cape Town, Atmospheric Environment, 87, 228-238, http://dx.doi.org/10.1016/j.atmosenv.2014.01.063, 2014.

Oltmans, S. J., Lefohn, A. S., Shadwick, D., Harris, J. M., Scheel, H. E., Galbally, I., Tarasick, D. W., Johnson, B. J., Brunke, E. G., Claude, H., Zeng, G., Nichol, S., Schmidlin, F., Davies, J., Cuevas, E., Redondas, A., Naoe, H., Nakano, T., and Kawasato, T.: Recent tropospheric ozone changes - A pattern dominated by slow or no growth, Atmospheric Environment, 67, 331-351, 10.1016/j.atmosenv.2012.10.057, 2013.

Parrish, D. D., Law, K. S., Staehelin, J., Derwent, R., Cooper, O. R., Tanimoto, H., Volz-Thomas, a., Gilge, S., Scheel, H. E., Steinbacher, M., and Chan, E.: Long-term changes in lower tropospheric baseline ozone concentrations at northern mid-latitudes, Atmospheric Chemistry and Physics, 12, 11485-11504, 10.5194/acp-12-11485-2012, 2012.

Parrish, D. D., Law, K. S., Staehelin, J., Derwent, R., Cooper, O. R., Tanimoto, H., Volz-Thomas, a., Gilge, S., Scheel, H. E., Steinbacher, M., and Chan, E.: Lower tropospheric ozone at northern midlatitudes: Changing seasonal cycle, Geophysical Research Letters, 40, 1631-1636, 10.1002/grl.50303, 2013.

Rahn, D. a., and Garreaud, R. D.: A synoptic climatology of the near-surface wind along the west coast of South America, International Journal of Climatology, 34, 780-792, 10.1002/joc.3724, 2014.

Reich, P. B., and Amundson, R. G.: Ambient levels of ozone reduce net photosynthesis in tree and crop species, Science (New York, N.Y.), 230, 566-570, 10.1126/science.230.4725.566, 1985.

Rondanelli, R., Gallardo, L., and Garreaud, R. D.: Rapid changes in ozone mixing ratios at Cerro Tololo (30°10′S, 70°48′W, 2200 m) in connection with cutoff lows and deep troughs, Journal of Geophysical Research: Atmospheres, 107, 1-15, 10.1029/2001JD001334, 2002.

Rutllant, J. A., Muñoz, R. C., and Garreaud, R. D.: Meteorological observations on the northern Chilean coast during VOCALS-REx, Atmos. Chem. Phys., 13, 3409-3422, 10.5194/acp-13-3409-2013, 2013.

Sekiya, T., and Sudo, K.: Role of meteorological variability in global tropospheric ozone during 1970–2008, Journal of Geophysical Research: Atmospheres, 117, n/a-n/a, 10.1029/2012JD018054, 2012.

Shi, Y., and Yamaguchi, Y.: A high-resolution and multi-year emissions inventory for biomass burning in Southeast Asia during 2001–2010, Atmospheric Environment, 98, 8-16, http://dx.doi.org/10.1016/j.atmosenv.2014.08.050, 2014.

Sillman, S., and He, D.: Some theoretical results concerning O3-NOx-VOC chemistry and NOx-VOC indicators, Journal of Geophysical Research: Atmospheres, 107, ACH 26-21-ACH 26-15, 10.1029/2001JD001123, 2002.

Škerlak, B.: Climatology and process studies of tropopause folds , cross-tropopause exchange , and transport into the boundary layer, Dissertation, ETH ZURICH, 2014.

Škerlak, B., Sprenger, M., and Wernli, H.: A global climatology of stratosphere-troposphere exchange using the ERA-Interim data set from 1979 to 2011, Atmospheric Chemistry and Physics, 14, 913-937, 10.5194/acp-14-913-2014, 2014.

Sofen, E. D., Bowdalo, D., and Evans, M. J.: How to most effectively expand the global surface ozone observing network, Atmos. Chem. Phys., 16, 1445-1457, 10.5194/acp-16-1445-2016, 2016a.

Sofen, E. D., Bowdalo, D., Evans, M. J., Apadula, F., Bonasoni, P., Cupeiro, M., Ellul, R., Galbally, I. E., Girgzdiene, R., Luppo, S., Mimouni, M., Nahas, A. C., Saliba, M., and Tørseth, K.: Gridded global surface ozone metrics for atmospheric chemistry model evaluation, Earth Syst. Sci. Data, 8, 41-59, 10.5194/essd-8-41-2016, 2016b.

Sprenger, M., and Wernli, H.: The LAGRANTO Lagrangian analysis tool – version 2.0, Geosci. Model Dev., 8, 2569-2586, 10.5194/gmd-8-2569-2015, 2015.

Staehelin, J., Harris, N. R. P., Appenzeller, C., and Eberhard, J.: Ozone trends: A review, 231-290, 2001.

Stevenson, D. S., Dentener, F. J., Schultz, M. G., Ellingsen, K., van Noije, T. P. C., Wild, O., Zeng, G., Amann, M., Atherton, C. S., Bell, N., Bergmann, D. J., Bey, I., Butler, T., Cofala, J., Collins, W. J., Derwent, R. G., Doherty, R. M., Drevet, J., Eskes, H. J., Fiore, a. M., Gauss, M., Hauglustaine, D. a., Horowitz, L. W., Isaksen, I. S. a., Krol, M. C., Lamarque, J. F., Lawrence, M. G., Montanaro, V., Müller, J. F., Pitari, G., Prather, M. J., Pyle, J. a., Rast, S., Rodriquez, J. M., Sanderson, M. G., Savage, N. H., Shindell, D. T., Strahan, S. E., Sudo, K., and Szopa, S.: Multimodel ensemble simulations of present-day and near-future tropospheric ozone, Journal of Geophysical Research: Atmospheres, 111, 10.1029/2005JD006338, 2006.

Stohl, A., Wotawa, G., Seibert, P., and Kromp-Kolb, H.: Interpolation Errors in Wind Fields as a Function of Spatial and Temporal Resolution and Their Impact on Different Types of Kinematic Trajectories, Journal of Applied Meteorology, 34, 2149-2165, doi:10.1175/1520-0450(1995)034<2149:IEIWFA>2.0.CO;2, 1995.

Streets, D. G., Yarber, K. F., Woo, J. H., and Carmichael, G. R.: Biomass burning in Asia: Annual and seasonal estimates and atmospheric emissions, Global Biogeochemical Cycles, 17, n/a-n/a, 10.1029/2003GB002040, 2003.

Sudo, K., and Akimoto, H.: Global source attribution of tropospheric ozone: Long-range transport from various source regions, Journal of Geophysical Research: Atmospheres, 112, n/a-n/a, 10.1029/2006JD007992, 2007.

Thompson, A. M.: Southern Hemisphere Additional Ozonesondes (SHADOZ) 1998–2000 tropical ozone climatology 2. Tropospheric variability and the zonal wave-one, Journal of Geophysical Research, 108, 1998-2000, 10.1029/2002JD002241, 2003.

Thompson, A. M., Witte, J. C., Smit, H. G. J., Oltmans, S. J., Johnson, B. J., Kirchhoff, V. W. J. H., and Schmidlin, F. J.: Southern Hemisphere Additional Ozonesondes (SHADOZ) 1998-2004 tropical ozone climatology: 3. Instrumentation, station-to-station variability, and evaluation with simulated flight profiles, Journal of Geophysical Research: Atmospheres, 112, 1998-2004, 10.1029/2005JD007042, 2007.

Thompson, a. M., Balashov, N. V., Witte, J. C., Coetzee, J. G. R., Thouret, V., and Posny, F.: Tropospheric ozone increases over the southern Africa region: bellwether for rapid growth in Southern Hemisphere pollution?, Atmospheric Chemistry and Physics, 14, 9855-9869, 10.5194/acp-14-9855-2014, 2014.

Thoning, K. W., Tans, P. P., and Komhyr, W. D.: Atmospheric carbon dioxide at Mauna Loa Observatory: 2. Analysis of the NOAA GMCC data, 1974–1985, Journal of Geophysical Research, 94, 8549-8549, 10.1029/JD094iD06p08549, 1989.

Verma, S. K., Kawamura, K., Chen, J., Fu, P., and Zhu, C.: Thirteen years of observations on biomass burning organic tracers over Chichijima Island in the western North Pacific: An outflow region of Asian aerosols, Journal of Geophysical Research: Atmospheres, 120, 4155-4168, 10.1002/2014JD022224, 2015.

Volz, A., and Kley, D.: Evaluation of the Montsouris series of ozone measurements made in the nineteenth century, 332, 240-242, 10.1038/332240a0, 1988.

Wang, Y., Jacob, D. J., and Logan, J. A.: Global simulation of tropospheric O3-NO x -hydrocarbon chemistry: 3. Origin of tropospheric ozone and effects of nonmethane hydrocarbons, Journal of Geophysical Research: Atmospheres, 103, 10757-10767, 10.1029/98JD00156, 1998a.

Wang, Y., Logan, J. A., and Jacob, D. J.: Global simulation of tropospheric O3-NO x -hydrocarbon chemistry: 2. Model evaluation and global ozone budget, Journal of Geophysical Research: Atmospheres, 103, 10727-10755, 10.1029/98JD00157, 1998b.

Wespes, C., Hurtmans, D., Emmons, L. K., Safieddine, S., Clerbaux, C., Edwards, D. P., and Coheur, P. F.: Ozone variability in the troposphere and the stratosphere from the first 6 years of IASI observations (2008–2013), Atmos. Chem. Phys., 16, 5721-5743, 10.5194/acp-16-5721-2016, 2016.

Winer, A. M., Arey, J., Atkinson, R., Aschmann, S. M., Long, W. D., Morrison, C. L., and Olszyk, D. M.: Emission rates of organics from vegetation in California's Central Valley, Atmospheric Environment. Part A. General Topics, 26, 2647-2659, http://dx.doi.org/10.1016/0960-1686(92)90116-3, 1992.

Wu, Z., and Huang, N. E.: Ensemble Empirical Mode Decomposition: A noise-assisted data analysis method, Advances in Adaptive Data Analysis, 01, 1-41, doi:10.1142/S1793536909000047, 2009.

Ziemke, J. R., Chandra, S., Oman, L. D., and Bhartia, P. K.: A new ENSO index derived from satellite measurements of column ozone, Atmos. Chem. Phys., 10, 3711-3721, 10.5194/acp-10-3711-2010, 2010.

Surface ozone in the southern hemisphere: 20 years of data from a site with a unique setting in El Tololo, Chile, 30°N, 71°W, 2200 m asl

Julien G. Anet[1,2], Martin Steinbacher[1], Laura Gallardo[3,4], Patricio A. Velásquez Álvarez[5,6], Lukas Emmenegger[1], Brigitte Buchmann[1]

[1]Laboratory for Air Pollution / Environmental Technology, Swiss Federal Laboratories for Materials Science and Technology, Duebendorf, Switzerland
[2] WSL Institute for Snow and Avalanche Research SLF, Davos, Switzerland
[3]Departamento de Geofísica de la Universidad de Chile, Blanco Encalada 2002, piso 4, Santiago, Chile
[4]Center for Climate and Resilience Research (CR2), Blanco Encalada 2002, Santiago, Chile
[5]Dirección Meteorológica de Chile, Av. Portales 3450, Estación Central, Santiago, Chile
[6]Climate and Environmental Physics, Physics Institute, University of Bern, Bern, Switzerland

Correspondence to: Julien G. Anet (julien.anet@~~empa~~slf.ch)

S1: Comparison between TECO 49 (DMC) and TE49C (Empa)

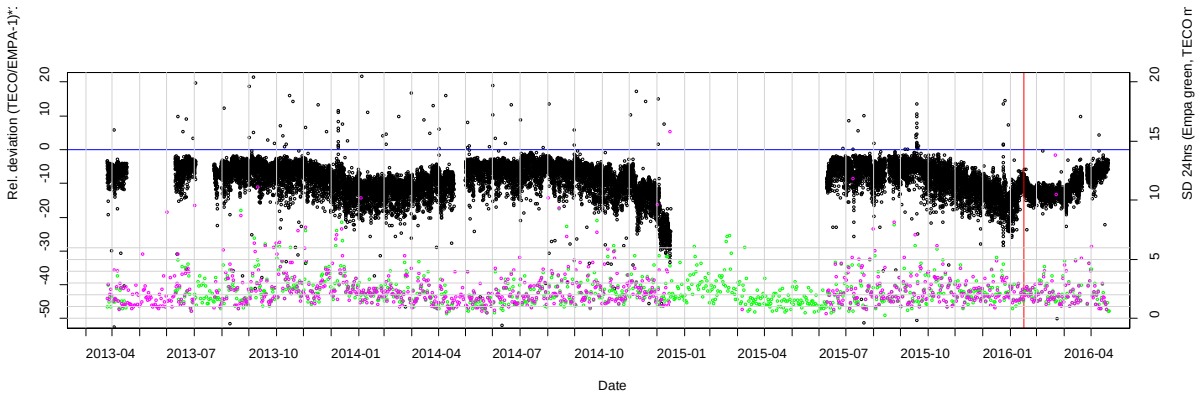

Fig. S1: Relative deviation of ozone measurements between TECO 49 and TE49C. Negative values (below blue line) show higher values measured with TE49C. Coloured points illustrate the 1-day standard deviation of measurements done either with the TECO 49 (magenta) or TE49C (green). Red line shows the time when the inlet tubing of the TECO 49 was replaced.

Since late April 2013, ozone at TLL has been measured in parallel with the TECO 49 from DMC and with the TE49C installed by Empa. Already in the beginning, a slight offset of 8-10% was noticed (equivalent to 2-3 ppb during average conditions at TLL). A more in-depth analysis revealed an annual cycle of the relative deviation ranging between 5 and 15% (equivalent to around 2 and 4 ppb), where the TECO 49 device always measured less ozone than the TE49C.

From mid-January 2015 to mid-June 2015, a series of failures interrupted the measurements of the TECO 49.

In late January 2016, the inlet tubing of the TECO 49 inlet was replaced, as it was speculated that the low readings were due to ozone losses at the inner surfaces of the aged (and possibly slightly soiled) tubing. No change in the differences could be observed after the change of the inlet tubing indicating that the aging of the tubing did not cause the losses and progressively growing losses over the years are unlikely. Presumably, the small systematic offset

is due to different inlet heights above ground and the different exposure of the intakes. The intake of the inlet for the TECO 49 is 2 m above ground whole the TE49C intake is at 5 m above ground.

S2: Filtering example

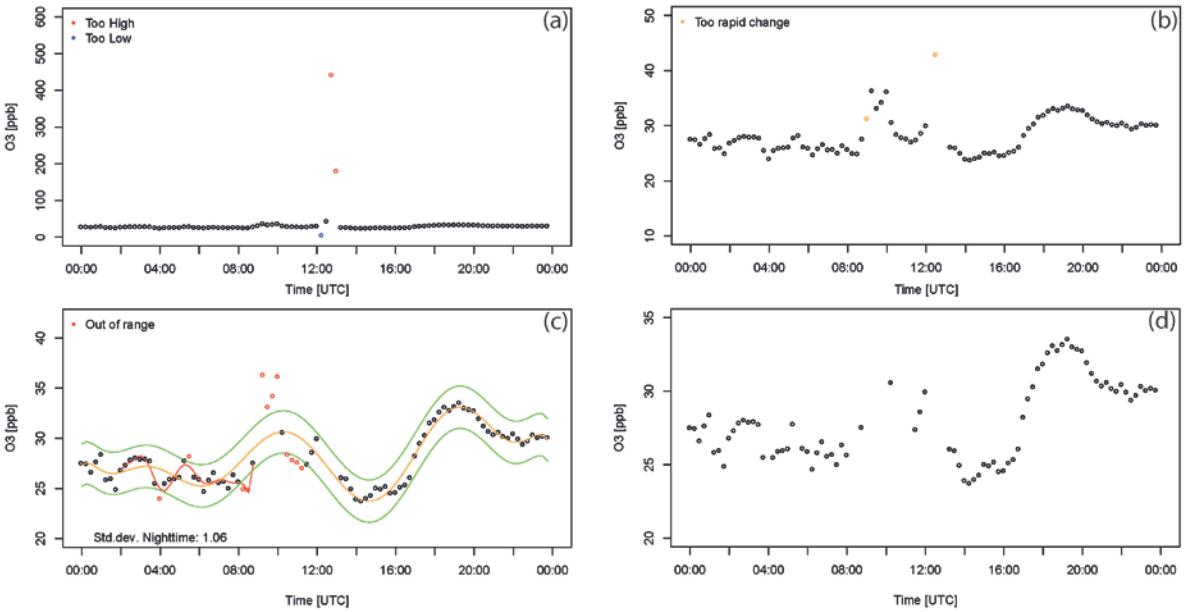

Fig. S2: Example of a typical filtering sequence, using original TECO 49 data from El Tololo between January 10th 2015 and January 11th 2015, UTC times. In a to d, the different steps are illustrated: a) Filtering out too high (red) and too low values (blue), b) Filtering too rapid changes (orange), c) Filtering out values exceeding twice the standard deviation (green curve, red points) computed over the polynomial fit during nighttime (23 to 6 LT, red curve), d) Final result.

S3: Additional figures

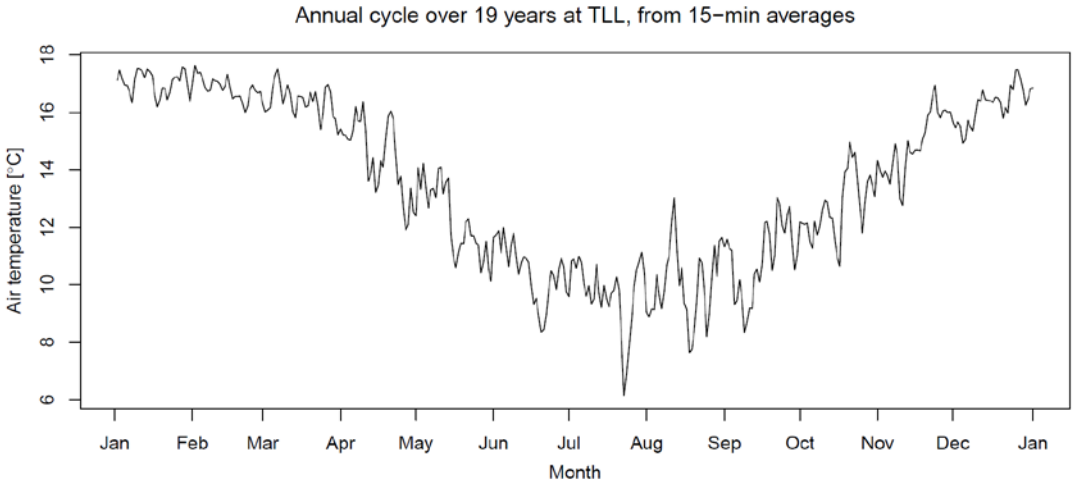

Fig. S3: Seasonal cycle of temperature over one year, computed as average over 19 years.

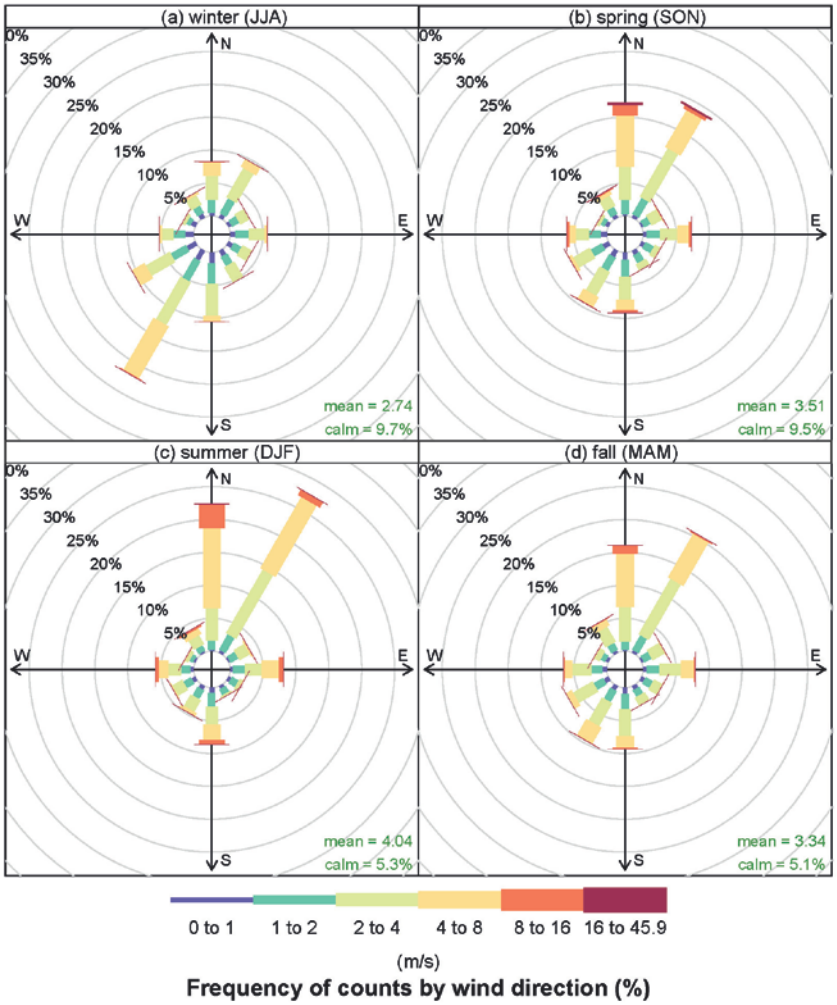

Fig. S4 Wind climatology 1995-2014 at El Tololo (DMC) for four seasons: (a) winter, (b) spring, (c) summer, (d) fall

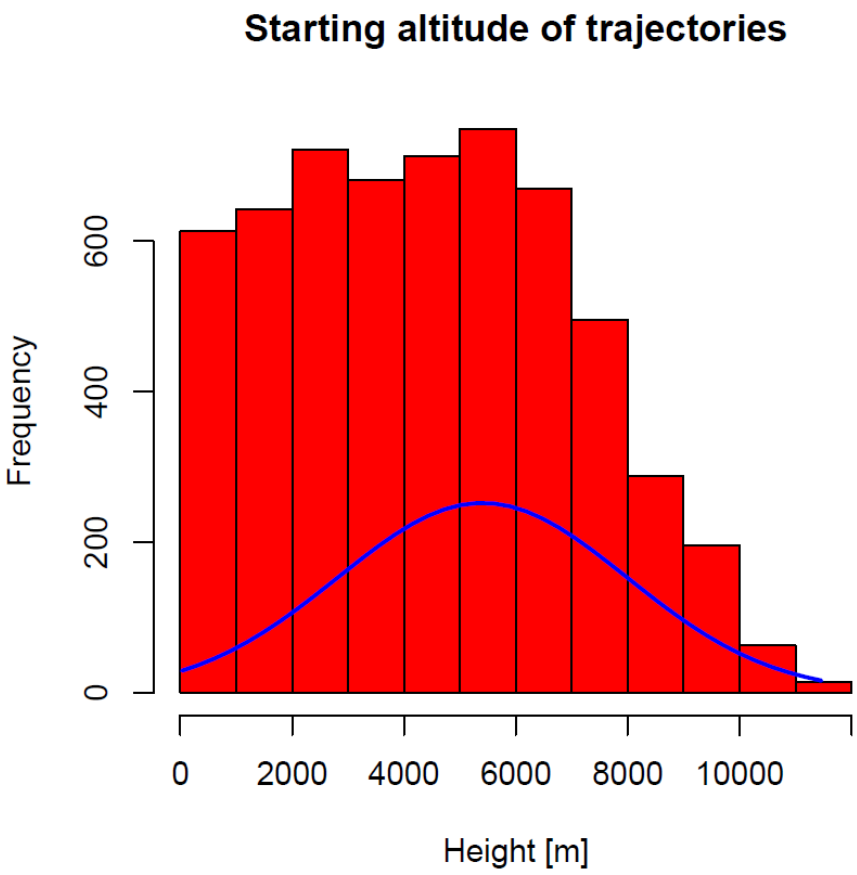

Fig. S5: Starting altitude distribution of the trajectories reaching TLL at a height of 370m.

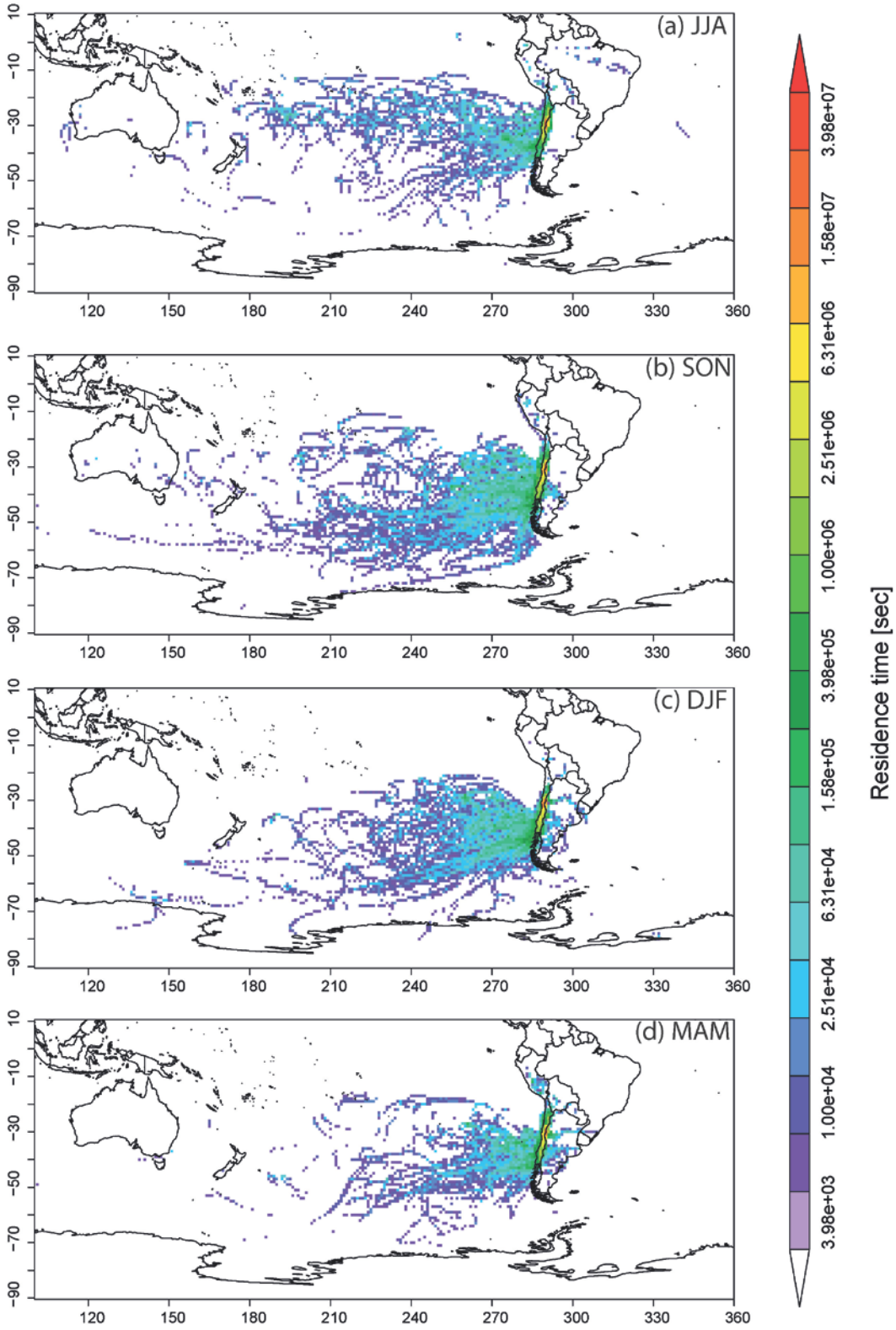

Figs. S6: FLEXTRA trajectory footprint from April 2013- December 2015, origin: TLL, 370m above model topography. Colour indicates the total residence time of air parcels, summed up over the time period. a) JJA, b) SON, c) DJF, d) MAM.

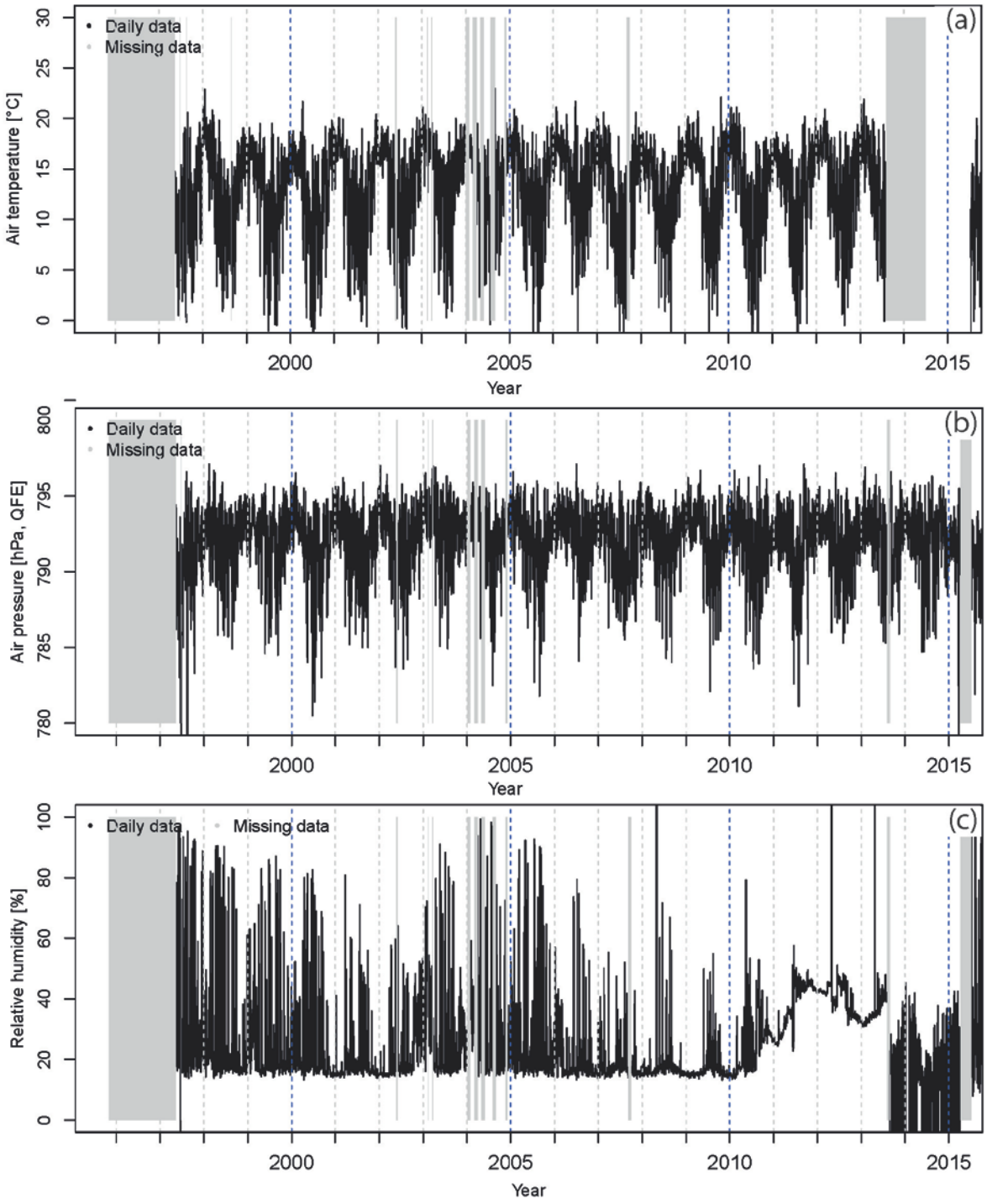

Fig. S7: Time series of a) air temperature, b) ambient pressure and c) relative humidity. Not available data is marked with grey lines.

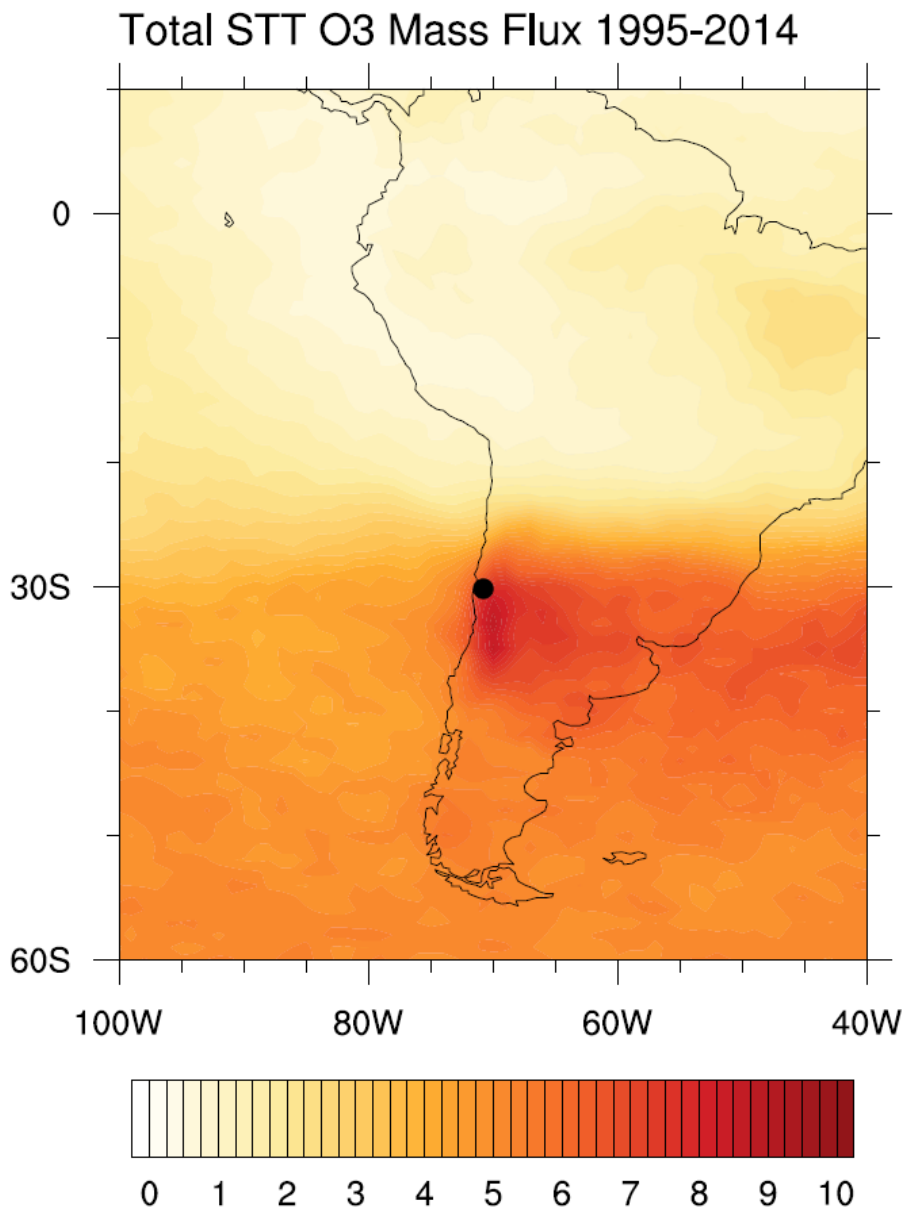

Fig. S8: Ozone Mass flux from the Stratosphere into the PBL, averaged from 1995 to 2014.

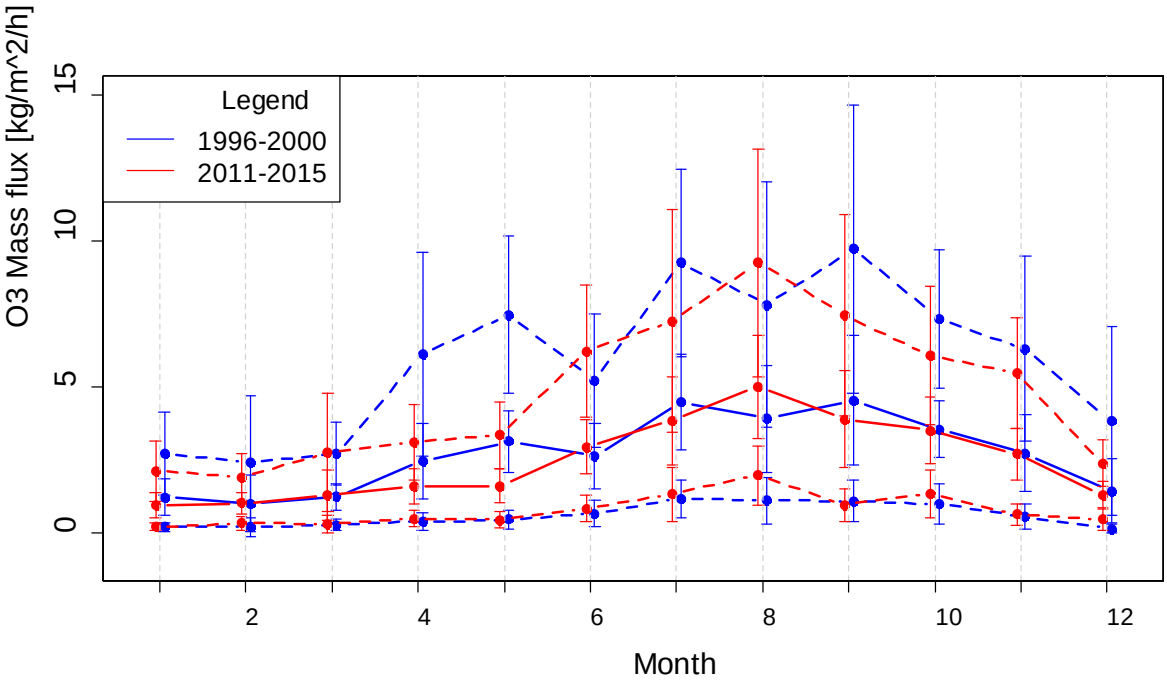

Fig. S9: Mean annual ozone STE~~T~~ mass flux cycle (1995-2000 and 2010-2015) showing mean, upper 95th percentile and lower 5th percentile.

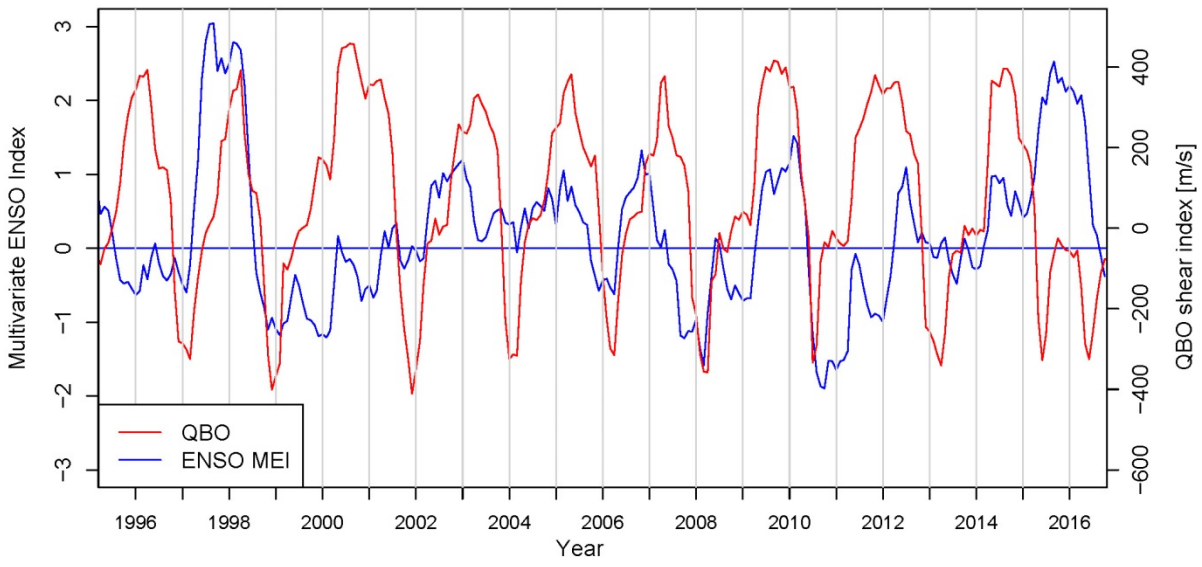

Fig. S10: QBO shear index (zonal wind at 50hPa-zonal wind at 25hPa) and MEI for the entire analysis period.

Table S 1: List of documented extended data gaps and their reasons.

Start of gap	End of gap	Reason
09.07.1999	14.07.1999	Power outage, no UPS available
09.12.1999	17.12.1999	Repainting of the measurement hut, data flagged.
12.08.2000	25.08.2000	Power outage, no UPS available
27.09.2001	10.10.2001	Internal pump failed
24.05.2002	04.04.2003	Internal pump failed, equipment is sent to DMC and repaired
21.10.2006	31.03.2007	Equipment is sent to Argentina for performance assessment (WCC-Empa)
03.09.2010	02.10.2010	Equipment is shipped to DMC for maintenance
06.08.2013	24.08.2013	Data logger failed
15.01.2015	23.04.2015	Internal pump failed
23.04.2015	19.06.2015	UV lamp failed